AD-A095 358   CALSPAN CORP BUFFALO NY   F/G 4/2

FOG CHARACTERISTICS AT OTIS AFB, MASSACHUSETTS.(U)

OCT 80 E J MACK, B J WATTLE, C W ROGERS   F19628-80-C-0041

UNCLASSIFIED CALSPAN-6655-M-1   AFGL-TR-80-0340   NL

1 OF 1
AD
A095358

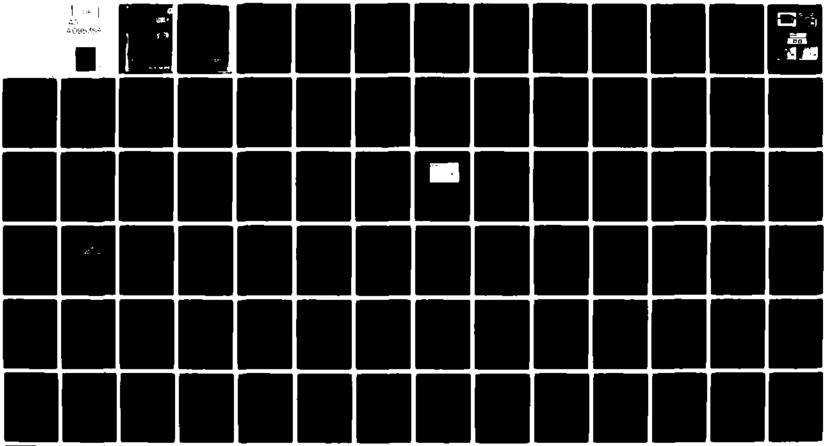

END
DATE
FILMED
3 81
DTIC

AFGL-TR-80-0340

FOG CHARACTERISTICS AT OTIS AFB, MA

E.J. Mack
B.J. Wattle
C.W. Rogers
R.J. Pilié

Calspan Corporation
P.O. Box 400
Buffalo, New York 14225

October 1980

Final Report
1 January 1980 - 30 September 1980

Approved for public release; distribution unlimited

AIR FORCE GEOPHYSICS LABORATORY
AIR FORCE SYSTEMS COMMAND
UNITED STATES AIR FORCE
HANSCOM AFB, MASSACHUSETTS 01731

(9) Final rept. 1 Jan-30 Sep 80

Unclassified

SECURITY CLASSIFICATION OF THIS PAGE (When Data Entered)

(19) REPORT DOCUMENTATION PAGE

READ INSTRUCTIONS BEFORE COMPLETING FORM

1. REPORT NUMBER: (18) AFGL-TR-80-0340	2. GOVT ACCESSION NO.: AD-A095358	3. RECIPIENT'S CATALOG NUMBER
4. TITLE (and Subtitle): (6) Fog Characteristics at Otis AFB, ~~Ma.~~ Massachusetts.		5. TYPE OF REPORT & PERIOD COVERED: Final Report 1/1/80 - 9/30/80
		6. PERFORMING ORG. REPORT NUMBER: 6655-M-1
7. AUTHOR(s): (10) E.J. Mack, B.J. Wattle, C.W. Rogers, R.J. Pilie		8. CONTRACT OR GRANT NUMBER(s): (15) F19628-80-C-0041 new
9. PERFORMING ORGANIZATION NAME AND ADDRESS: Calspan Corporation, PO Box 400, Buffalo, NY 14225		10. PROGRAM ELEMENT, PROJECT, TASK AREA & WORK UNIT NUMBERS: 62101F (16) 667010AK (17) 10
11. CONTROLLING OFFICE NAME AND ADDRESS: Air Force Geophysics Laboratory, Hanscom AFB, Massachusetts 01731, Monitor/Bruce A. Kunkel/LYU (11)		12. REPORT DATE: October 1980
		13. NUMBER OF PAGES: 83
14. MONITORING AGENCY NAME & ADDRESS (if different from Controlling Office): (12) 83		15. SECURITY CLASS. (of this report): Unclassified
		15a. DECLASSIFICATION DOWNGRADING SCHEDULE

16. DISTRIBUTION STATEMENT (of this Report)

Approved for public release; distribution unlimited.

(14) CALSPAN-6655-M-1

17. DISTRIBUTION STATEMENT (of the abstract entered in Block 20, if different from Report)

18. SUPPLEMENTARY NOTES

19. KEY WORDS (Continue on reverse side if necessary and identify by block number)

Fog	CCN
Fog microphysics	Dew deposition
Aerosol size spectra	Otis AFB
Aerosol composition	Cape Cod

20. ABSTRACT (Continue on reverse side if necessary and identify by block number)

Measurements of the microphysical characteristics of fog occurring at Otis AFB (Cape Cod) were obtained during a three-week field study in July 1980. Measurements of dew deposition, CCN and pre-fog aerosol size spectra and samples of aerosols for composition analysis were also acquired. Results of the analyses and limited interpretation of the data are presented.

DD FORM 1 JAN 73 1473 EDITION OF 1 NOV 65 IS OBSOLETE

Unclassified

SECURITY CLASSIFICATION OF THIS PAGE (When Data Entered)

407727

TABLE OF CONTENTS

LIST OF FIGURES

LIST OF TABLES

Section 1
INTRODUCTION

Under Contract No. F19628-80-C-0041 from the Air Force Geophysics Laboratory (AFGL), Air Force Systems Command, Calspan assisted AFGL in the comparison of fog droplet sizing instrumentation and in the acquisition of droplet size, condensation nuclei and other microphysical and micrometeorological data in natural fogs occurring at the AFGL Weather Test Facility at Otis AFB, Massachusetts. The primary objective of this program was to obtain data for the comparison of the drop-size-measurement capability of an AFGL-owned PMS forward scattering probe (Model FSSP-100) and of a Spectron Development Laboratories (SDL) Particle Sizing Interferometer with that of Calspan's Droplet Sampler in simulated natural fogs produced in Calspan's 590 m^3 chamber and in natural fogs occurring at Otis AFB during July 1980. The SDL device was employed only for the chamber tests. In addition, measurements of visibility in the chamber tests and of liquid water content, aerosol size spectra, and condensation nublei at Otis were obtained to supplement the droplet size data.

Calspan's primary role in this program was to provide drop-size distribution, drop concentration and liquid water content data in both laboratory and natural fogs for comparison with data obtained with the aforementioned devices. In pursuit of this objective, joint AFGL-Calspan-SDL tests were conducted in laboratory fogs produced in Calspan's chamber. The test program was conducted during the period 4-6 March 1980; 12 fogs were produced for observation. By mutual agreement, Calspan drop-size data were reduced and analyzed for eight of those experiments, and the data were provided in an Interim Technical Report*. Due to instrumentation difficulties, SDL data were only available for four experiments. SDL's data were provided in a separate report**.

---

*Mack, E.J., 1980: "Collection and Reduction of Drop Size Distribution Data in Simulated and Natural Fogs: Chamber Fog Tests," Calspan Report, May 1980, 99 pp.

**Spectron Development Laboratories, Inc., 1980: "Study of Fog Formation Characteristics with a Droplet Sizing Interferometer," SDL Report No. 80-6577, May 1980, 80 pp.

The field measurements were made at the AFGL Weather Test Facility located at Otis AFB (Cape Cod) during the period 30 June to 18 July 1980. During the three-week field effort, a joint AFGL-Calspan team obtained measurements on a nightly basis from ∿2000 to 0500 EDT, and data were acquired in six deep advection fogs, two shallow ground fogs and four dense hazes (visibility 2-4 km). While Calspan's primary objective was measurement of droplet size spectra in fogs, we also obtained measurements of CCN concentrations, pre-fog aerosol size spectra, dew deposition, wind speed and direction, temperature and relative humidity, low-level air temperature profiles and soil temperatures, aerosol samples for composition (elemental) analysis, and records of visibility as measured by AFGL-owned EG&G Forward Scatter Meters at heights of 5, 30, 45 and 60 m above the surface.

The scope of Calspan's contract did not permit more than limited reduction of data other than fog microphysics and CCN, but the field program provided an opportunity for additional limited study of dew deposition, low-level air-soil temperature profiles, liquid water content profiles and the chemistry of ambient aerosols. These analyses were supported in part by Calspan IR&D Project No. 85-435 and in part by Scientific Services Agreement No. 1592 from the Atmospheric Sciences Laboratory, White Sands (through the Army Research Office and Battelle). The analyses and supporting data, where available, are provided within this report for completeness.

Instrumentation is described in Section 2.1, and the fogs, visibility and drop-size data are discussed in Section 2.2. Liquid water content profiles and dew deposition are discussed in Sections 2.3 and 2.4, respectively. Pre-fog aerosol characteristics, including CCN, size spectra and composition, are presented in Section 2.5. An hourly log of measured meteorological variables, where available for the nighttime hours of the field study, is provided in Appendix A. Droplet size spectra, air-soil temperature profile data, and pre-fog aerosol size spectra are provided for selected fogs in Appendices B, C and D, respectively.

Section 2

RESULTS OF THE FIELD MEASUREMENTS AT OTIS AFB

2.1 Instrumentation and Field Site

Calspan instrumentation was delivered to the AFGL Weather Test Facility site at Otis AFB, MA, late on 29 June 1980 and set up during the following two days. The primary site of the Facility comprises an "L"-shaped layout of five towers, three of which are 60 m high. Calspan's mobile laboratory was positioned at the base of one of these 60 m towers, adjacent to an AFGL van. Calspan instrumentation, listed in Table 1, was installed at various heights and locations on the tower, on the roof of the van and on the ground immediately surrounding the tower.

During the 20-day field study, measurements were obtained nightly during the period ∿2000 to ∿0500 EDT. The parameters measured in this study fell into three general categories: fog microphysics, pre-fog aerosol characteristics, and supporting meteorological variables. For fog microphysics, a Calspan drop sampler, a hi-vol LWC sampler, AFGL's Forward Scatter Meters and a Royco OPC were employed; except for the visibility monitors which operated continuously, the microphysics instrumentation was operated intermittently during fog at intervals of 10 to 30 minutes. Pre-fog aerosol measurements included size spectra (0.01-5.0 μm), extinction coefficient, CCN concentrations, and samples for chemical analyses; size spectra data were obtained at hourly intervals, extinction coefficient was monitored continuously, CCN were measured twice nightly, and aerosol samples via cascade impactor were obtained on eight nights. Monitored meteorological variables included wind speed and direction, visibility, air temperature at three heights below 1.0 m, ground temperature at the surface and at two depths, wet- and dry-bulb temperatures (relative humidity) and dew deposition; dew deposition and relative humidity were measured hourly and all other meteorological parameters were measured continuously. Pertinent Calspan instrumentation are described below, and an hourly log of measured meteorological variables, where available for the nighttime hours, is provided in Appendix A.

Table 1. Calspan Instrumentation Employed at Otis AFB

Instrument	Parameter	Measurement Height Above Surface
Calspan Drop Sampler (2) (gelatin replic.)	Fog drop size spectra (~4-50 μm dia) Drop Concentration Liquid Water Content	5 and 44 m
Hi-Vol LWC Sampler (2)	Liquid Water Content	5 and 44 m
Royco OPC	Aerosol Size Spectra (0.3-5.0 μm dia)	3 m
TSI Electrical Aer. Analyzer	Aerosol Size Spectra (0.01-0.7 μm dia)	3 m
MRI Integrating Nephelometer	Scattering Coefficient Visibility (2-80 km)*	3 m
Calspan Diffusion Chamber	CCN @ 0.2-1.0% S	3 m
Casella Cascade Impactor	Aerosol Samples for Chem. Anal.	1 m
Calspan Dewplates (2)	Dew Deposition	0.2 m
Calspan Temp System (6 sensors)	Ground Temperature Air Temperature	sfc, 2.0 and 6.0 cm below sfc 0.1, 0.4, 0.9 m above sfc
Sling Psychrometer	Wet- and Dry-Bulb Temp Relative Humidity	~1 m
Beckman/Whitley Wind System	Wind Speed and Direction	11.5 m

*Visibility in fog (60-6000 m) was measured by AFGL-owned EG&G Forward Scatter Meters at heights of 5, 30, 45 and 60 m on the tower, and strip chart records were acquired with recorders in Calspan's van.

- The Calspan Droplet Sampler

The Calspan Droplet Sampler, pictured in Figure 1, was used to obtain measurements of fog droplet size spectra. In operation, foggy air is drawn through a sampling tube by a high capacity blower, and droplets are collected by impaction on gelatin-coated slides. The sampling airspeed is measured by a pitot tube and static source mounted in the unit, and a standard aircraft airspeed indicator is used to read the airspeed through the sampler. Airspeed is adjustable from 20 to 80 m/sec, but typically an impaction velocity of ∿40 m/sec was used.

Droplet samples are taken by injecting a narrow, gelatin-coated, glass slide*, pictured in Figure 2, into the high speed flow through an opening in the sampling tube. Slide injection is accomplished through the use of a modified 35 mm photographic slide changer. When the coated slide is exposed to the air flow in the tube, droplets in the air volume swept out by the 4 mm wide glass slide impinge on the gelatin coating and form crater-like depressions such as shown at the bottom of Figure 2. Development work on this technique (Jiusto, 1965 and Mack, 1966)** has shown that there is approximately a 2:1 ratio between the crater diameter and the diameter of the impinging droplet. Exposure times are typically ∿0.2 sec, but can be extended to minutes as might be required for light hazes.

A fundamental source of error associated with the gelatin slide technique is caused by droplets following the air flow around the slide and not being collected. Impaction occurs on the slide only when droplets have

*Slides are prepared by mounting 4 mm wide glass strips in standard 35 mm photographic slide frames. After mounting, the glass is coated on one side with a 15% by weight gelatin solution. Up to 40 slides can be loaded into the sampler magazine and exposed in sequence.

**Jiusto, J.E., 1965: Cloud Particle Sampling, Pennsylvania State University, Department of Meteorology, Report No. 6, NSF G-24850.

Mack, E.J., 1966: "Techniques for Analysis of Cloud Particle Samples," Pennsylvania State University, Department of Meteorology, Report No. 14, NSF GP-4743.

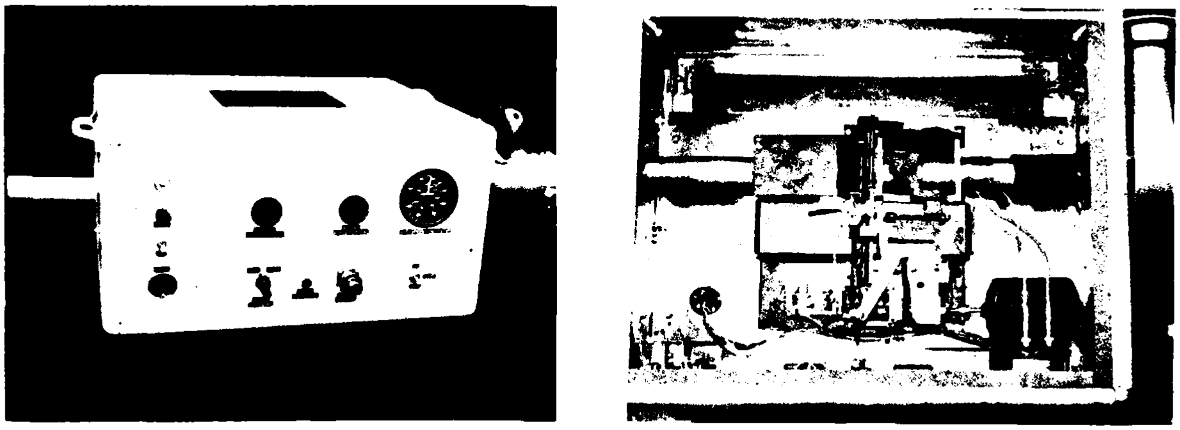

Figure 1 CALSPAN FOG DROPLET SAMPLER

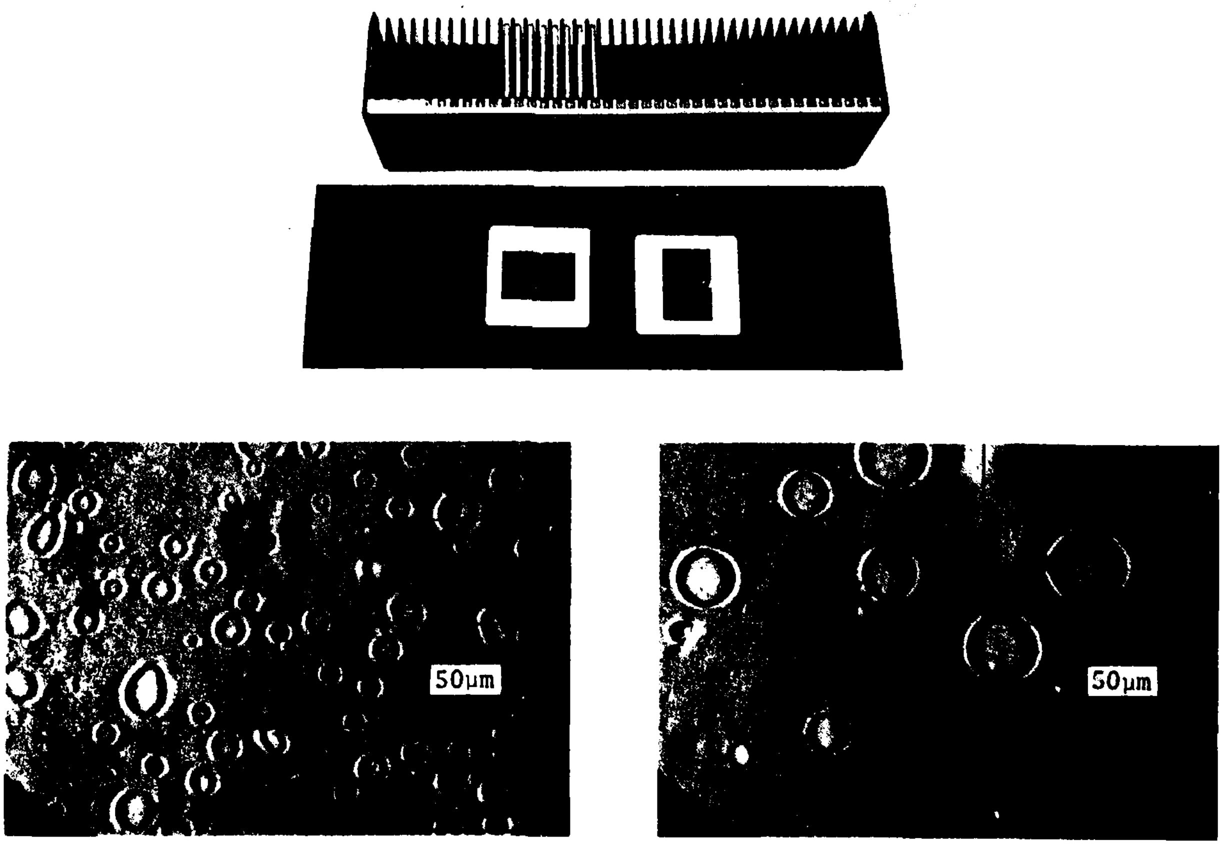

a) Radiation Fog   b) Advection Fog

Figure 2 SLIDE MAGAZINE, GELATIN-COATED SAMPLE SLIDES, AND DROPLET REPLICAS

sufficient momentum to deviate from the streamlines around the slide. Therefore, as droplet diameters get smaller and their momentum decreases, collection efficiency decreases. Collection efficiency can be expressed in terms of the ratio of effective slide width to actual slide width and is a function of droplet diameter, slide width and airspeed. Langmuir and Blodgett (1946)* investigated collection efficiencies of flat plates in some detail, and some computed collection efficiencies using their data for a collector slide of 4 mm width and airspeeds of 20 to 80 m/sec as shown below.

Collection Efficiencies of 4 mm Wide Slides
in the Calspan Droplet Sampler

	Droplet Radius (microns)							
Airspeed m/sec	1	2	3	4	5	6	8	10
20	.00	.37	.64	.75	.81	.86	.91	.94
40	.09	.59	.75	.83	.88	.91	.94	.96
60	.21	.68	.81	.87	.91	.93	.95	.97
80	.33	.72	.83	.89	.92	.94	.96	.97

For 4 mm wide slides and the sampling velocities of 40-60 m/sec typically employed in the drop sampler, it is seen that collection efficiencies are better than 75% for droplets larger than 3 μm radius and >90% for droplets larger than 5 μm radius. It should also be noted that collection falls off rapidly for droplets below 2 μm radius. This feature places a lower limit of about 2 μm radius on the drop sizes that can be sampled with any degree of confidence.

*Langmuir, I. and K.B. Blodgett, 1946: U.S. Army Air Force, Technical Report No. 5418.

Reduction of the droplet data is performed manually from photomicrographs (of the sample slides) obtained with a phase contrast microscope. Where possible, a minimum of 200 droplets is measured, with an accuracy of ±10% of drop radius, for each drop size distribution. Figure 2 illustrates the droplet data in raw form, showing photomicrographs of fog droplet samples. The indicated scale dimension on the figure is 1/2 the actual scale to account for the ratio of crater size to actual droplet size.

The raw distributions produced from measurements of the droplet replicas provide input to a computer program which first corrects for collection efficiency of the slide and then produces a normalized drop size distribution, $N(r_i)$, where $N(r_i)$ is the fraction of drops of radius r_i. Droplet concentration is then computed by using the measured extinction coefficient (β) and the expression

$$\beta = 2\pi n \sum N\,(r_i) r_i^{\,2} \tag{1}$$

where n = total number of drops per unit volume.

The computation of LWC, ω, is then straightforward, where

$$\omega = \frac{4\pi n}{3} \sum N\,(r_i) r_i^{\,3}. \tag{2}$$

Extinction coefficient, β in Eq. (1), was measured as "scattering" coefficient in fog at Otis with EG&G Forward Scatter Meters. The measured extinction can be related to visual range, V, through Koschmieder's expression

$$V = -\ln \varepsilon/\beta \tag{3}$$

where ε is the threshold contrast. Values of ε ranging from 0.01 to 0.06 have been proposed by a number of authors, however, Koschmeider defined meteorological visual range, Vm, as the atmospheric pathlength required to reduce apparent contrast, ε, to 0.02; hence, Eq. (3) reduces to $Vm = 3.912/\beta$. However, the manufacturer's calibration for the Forward Scatter Meter assumes $\varepsilon = 0.04745$ and, hence, $V = 3.048/\beta$; in-fog visibility data presented in Section 2.2 was calculated according to this latter relationship. For haze and "clear air" conditions, an MRI Integrating Nephelometer was employed. Visibility data from this device (Section 2.2, p.11 and Appendix A) was computed using the manufacturer's assumption and calibration; i.e., $\varepsilon = 0.01$ and $V = 4.605/\beta$.

- The Calspan Static Thermal Gradient Diffusion Chamber

The Calspan thermal gradient diffusion chamber has been used for making measurements of cloud nuclei (CCN) since 1964. The basic design of the chamber is patterned after that of Langsdorf (1936), Wieland (1956) and also Twomey (1963)**. In brief, the unit consists of a cylindrical plexiglass chamber with upper and lower water reservoirs, a servo-controlled cooling module beneath the lower reservoir, a collimated light beam to illuminate a small volume within the chamber, and a polaroid camera for photographing droplets that have formed on condensation nuclei.

During operation, water vapor diffuses from the warmer upper surface to the lower reservoir, with the chamber supersaturation being a known function of temperature difference (servo-controlled) between the two reservoirs. A series of 10 thermocouples (five on each surface) is used to measure ΔT. When the desired supersaturation has been achieved, an air sample containing nuclei to be investigated is drawn into the chamber at a continuous rate for several

---

*Pilié, R.J., Mack, E.J., Kocmond, W.C., Eadie, W.M., and Rogers, C.W., 1975: "The Life Cycle of Valley Fog: Part II - Fog Microphysics," J. Appl. Met. 14.

**Langsdorf, A., 1936: "A Continuously Sensitive Cloud Chamber," Phys. Rev. 49, p 422.

Wieland, W., 1956: "Condensation of Water Vapor on Natural Aerosol at Slight Supersaturation," Z. Agnew. Math. U. Phys. 7, pp 428-460.

Twomey, S., 1963: "Measurements of Natural Cloud Nuclei," J. Res. Atmos., I, 1, p 101.

seconds. The air sample is allowed to reside in the supersaturated environment where, in a few seconds, droplet growth proceeds on the most active condensation nuclei. The growing droplets are illuminated by a light beam of known dimensions (from a 200 watt Osram lamp) and photographed at 90° to the light beam moments before sedimentation begins.

The number of nuclei active at a given supersaturation is estimated from the photographs of particles activated to droplet growth by using a transparent overlay having dimensions of 0.5 cm x 1.0 cm. In practice, CCN activity spectra are drawn from ∿4 measurements obtained over a 10-15 minute interval and over a supersaturation range of ∿0.2% to 1.2%. Values at a specific supersaturation (i.e., 0.2, 0.5, 1.0% S) are read from these curves.

- The Calspan Dewplate

During our studies of fog in the late 1960's, we first became intrigued with the role of the heavy deposition of dew which usually preceded the formation of radiation and valley fogs. In an attempt to obtain quantitative estimates of the amount of dew on the ground, we constructed a dewplate consisting of a 0.05 m^2 aluminum plate mounted on a laboratory balance to measure dew deposition to ±0.1 g/0.05 m^2. In a later refinement, the balance was mounted inside a plexiglas box and a hinged cover was added to reduce wind effects during reading of the scales.

To reproduce the long-wave radiation characteristics of grass, the aluminum plate was painted black. This may not have been important since the surface of the plate was usually coated with dew within an hour after being placed in the field; and the radiating surface of the plate, like that of the grass, was usually water. Even so, the exact relationship between the dew deposition rates measured with this apparatus and deposition rates on ground/grass surfaces is unknown. Important differences probably include the six inch height of the plate above the ground and the ratio of the surface area exposed to the atmosphere to unit surface area of the ground. The surface area of vegetation in a meadow is given by Geiger (1965, Chapter V)* as 20 to 40 times the area of the ground. For the plate, of course, this ratio was very nearly two.

2.2 Fog Events Observed at Otis: Visibility and Drop Size Data

- Fog Occurrence and Visibility Data

During the approximate three-week field study, data were obtained in six deep advection fogs, two shallow ground fogs and four dense hazes. The advection fogs occurred during the nighttime hours of 1-2 July, 2-3 July, 3-4 July, 10-11 July, 11-12 July and 17-18 July with south to southwest winds. The occurrence of these fogs at the field site was apparently related to the afternoon sea breeze which advected evaporating offshore fog and marine air on shore. With onshore winds and diminishing solar heating in the late afternoon, relative humidity continuously increased while visibility gradually lowered at the field site. When sufficient cooling had occurred (between 1700 and 2000 EDT), visibility rapidly dropped below 6000 m at all measurement levels on the tower. During this formation stage of the fogs, lower visibilities were generally observed first at higher levels on the tower. Visibility data, where available for these six fogs**, are presented as functions of time and height in Figures 3-8. (See p. 8 for the relationship between extinction coefficient and visibility.)

Similarly, the dense hazes of the evenings of 8-9 July, 9-10 July, 14-15 July and 16-17 July, in which visibility degraded to <4 km (2.5 mi) but remained above ~ 2.5 km (1.5 mi), generally occurred with southwesterly winds but apparently in the absence of offshore fog. These hazes exhibited a marked dependence on wind direction, with visibility improvements occurring when winds veered to more westerly (and were no longer onshore). Hourly visibility data for these situations are tabulated in Appendix A.

---

*Geiger, R., 1965: The Climate Near the Ground, Harvard Univ. Press.

**Air-soil temperature profile data for some of these fogs may be found in Appendix C.

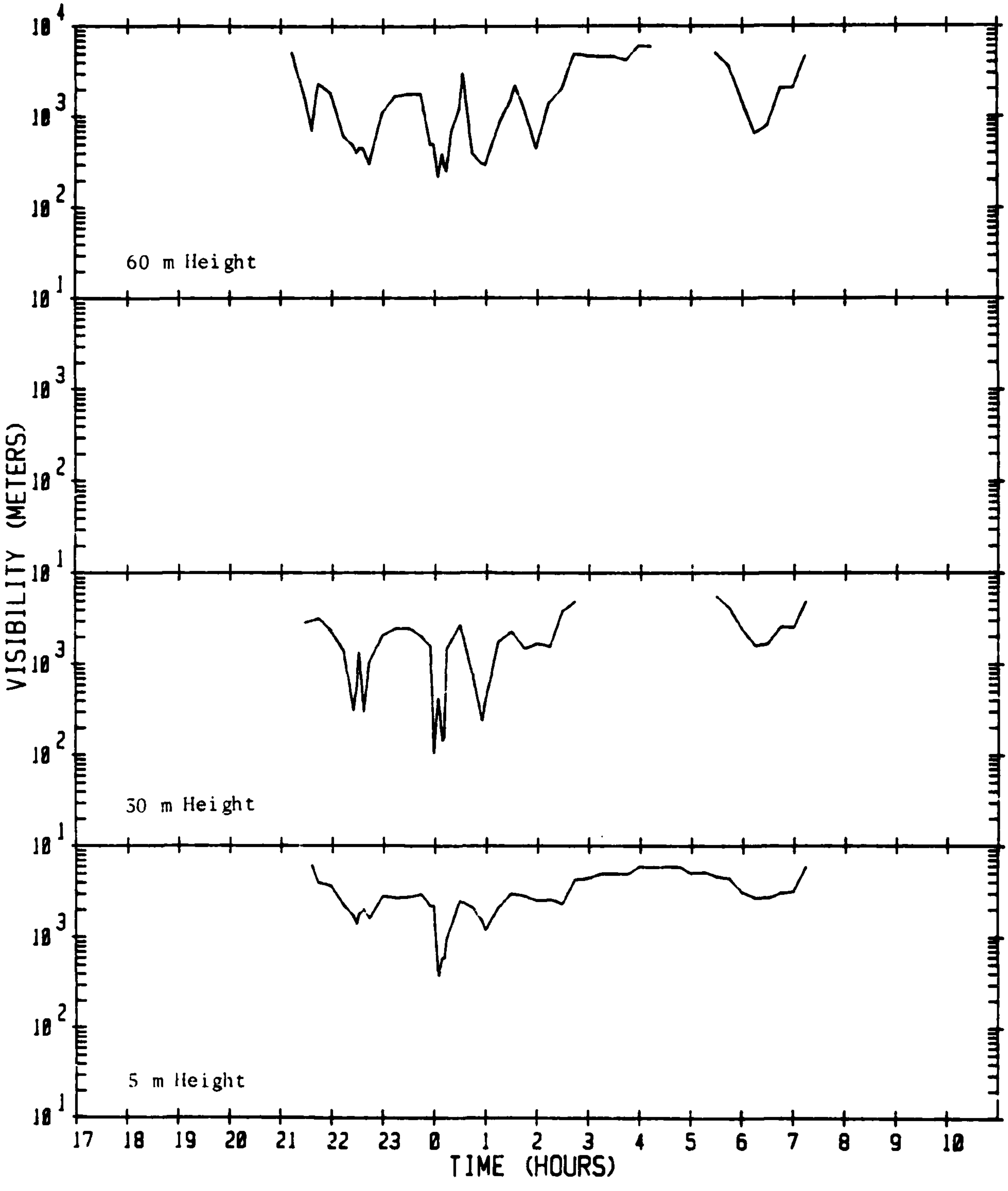

Figure 3. Visibility Records for Three Heights in the Fog of 1-2 July 1980

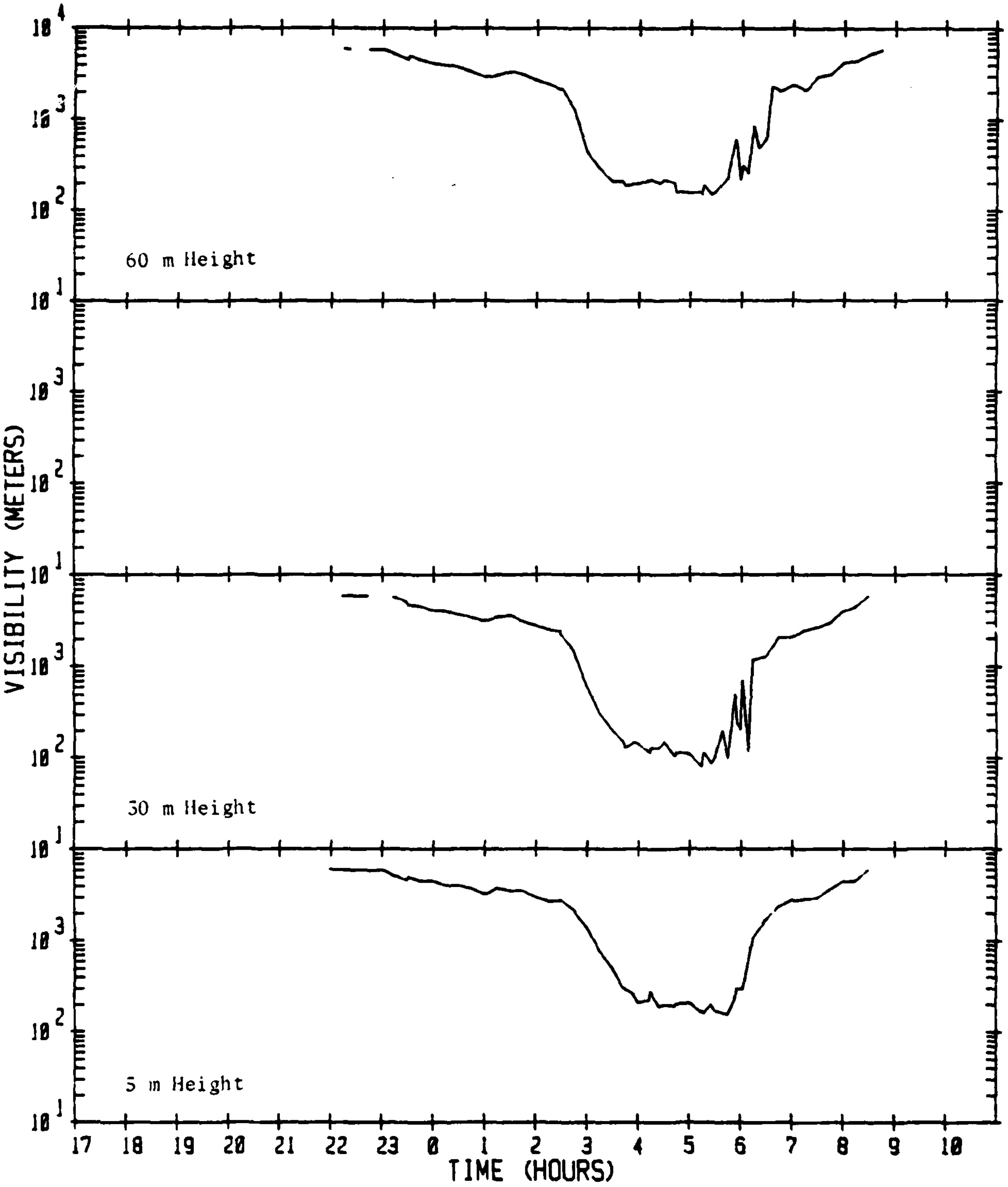

Figure 4. Visibility Records for Three Heights in the Fog of 2-3 July 1980

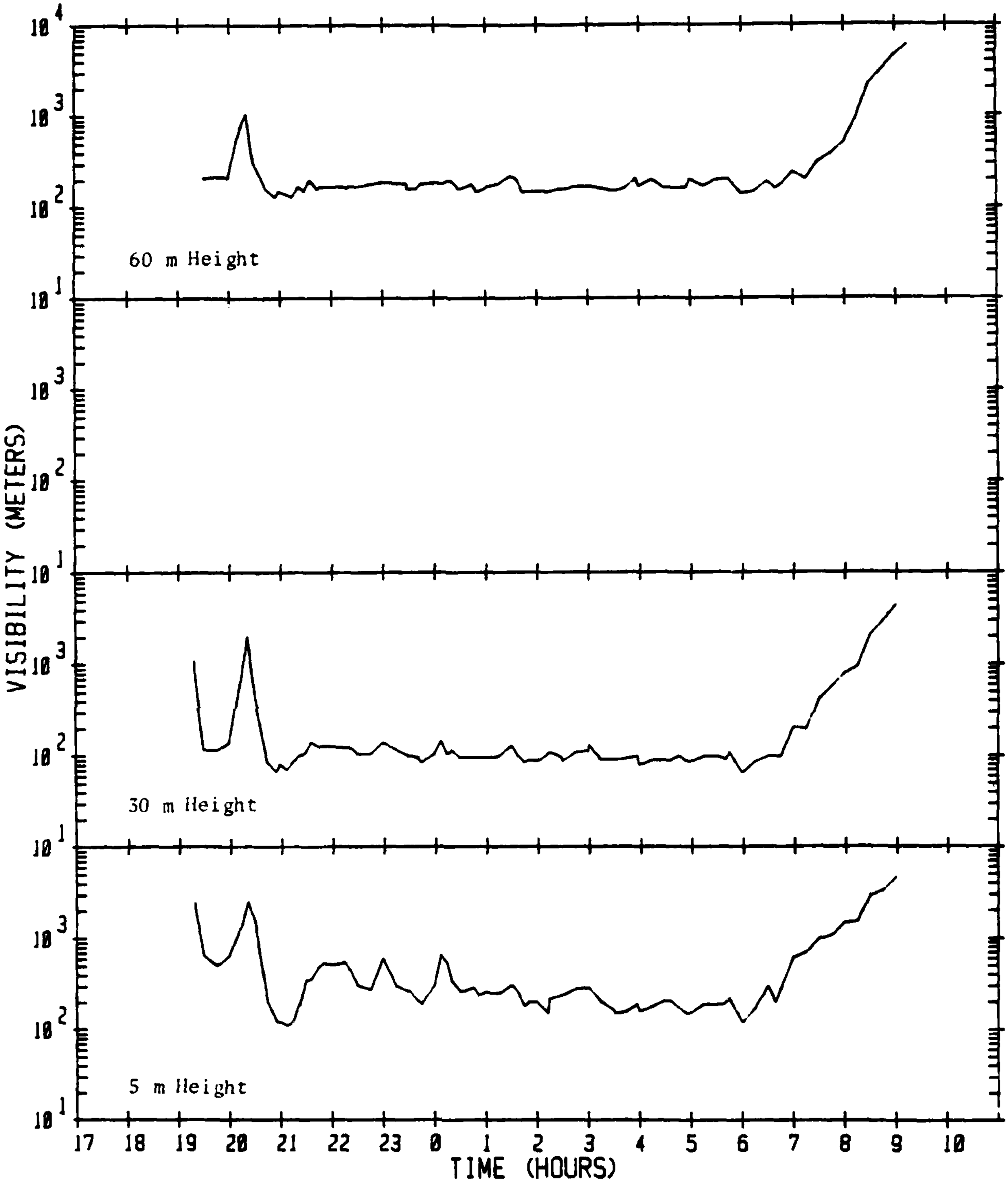

Figure 5. Visibility Records for Three Heights in the Fog of 3-4 July 1980

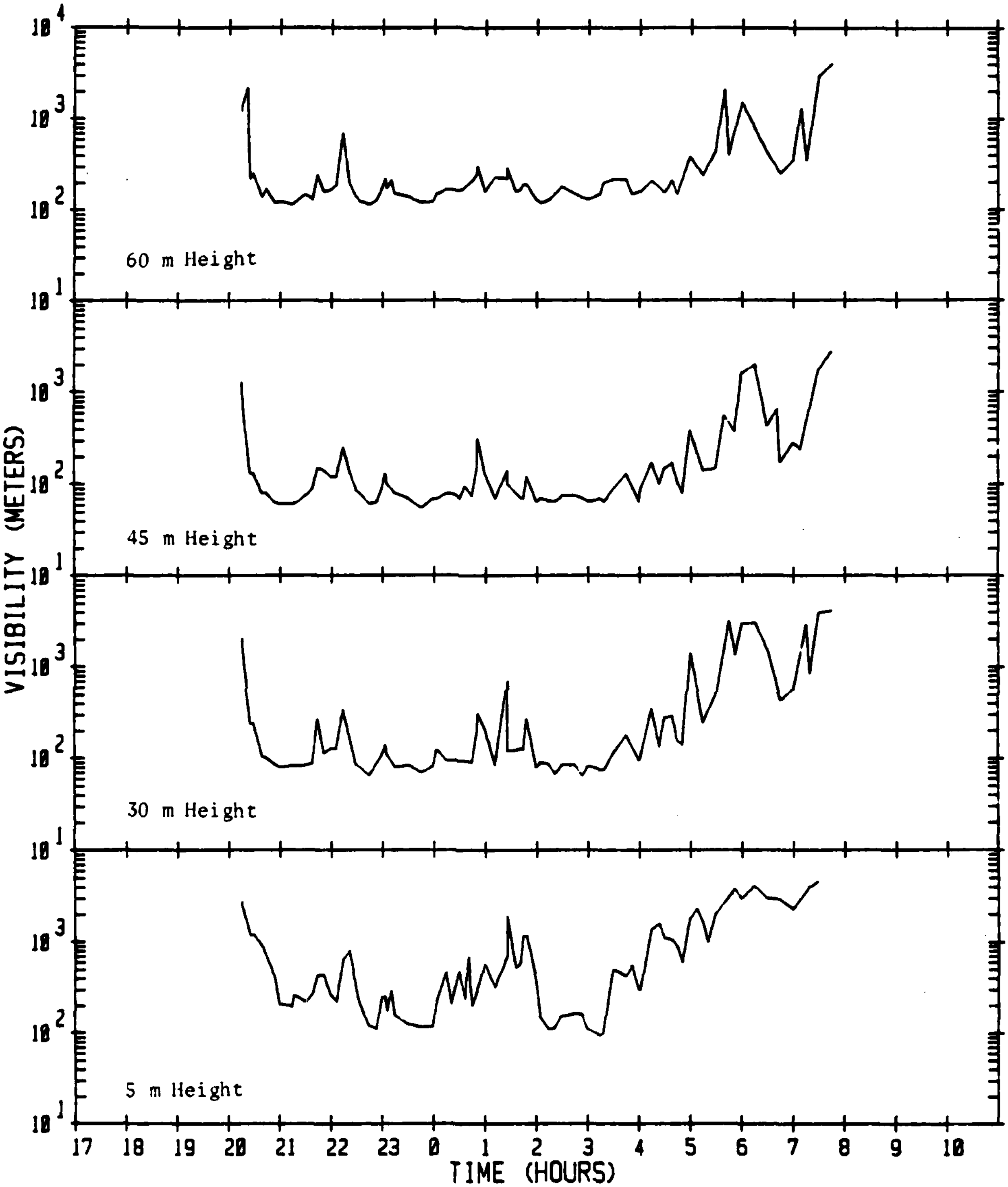

Figure 6. Visibility Records for Four Heights in the Fog of 10-11 July 1980

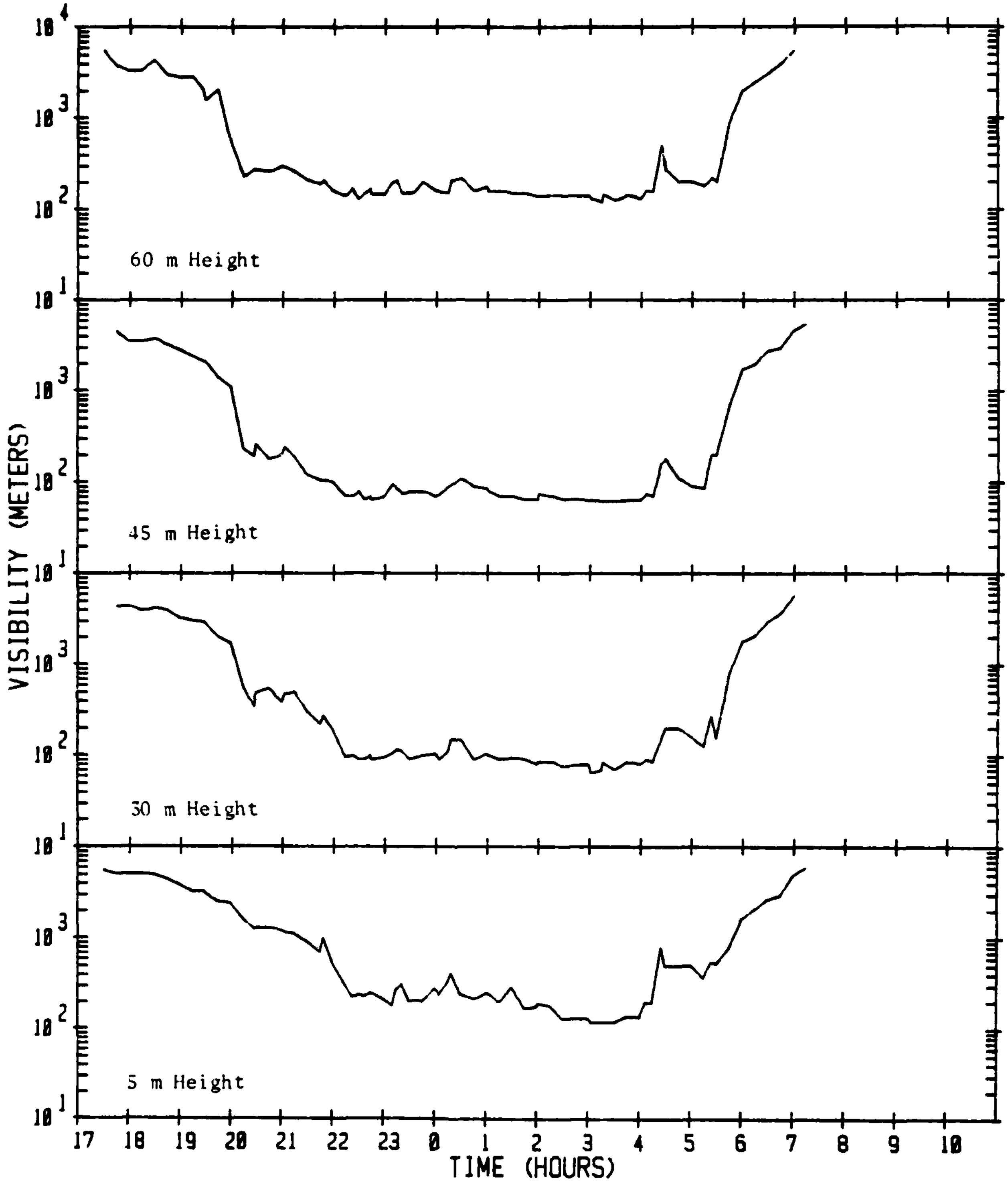

Figure 7. Visibility Records for Four Heights in the Fog of 11-12 July 1980

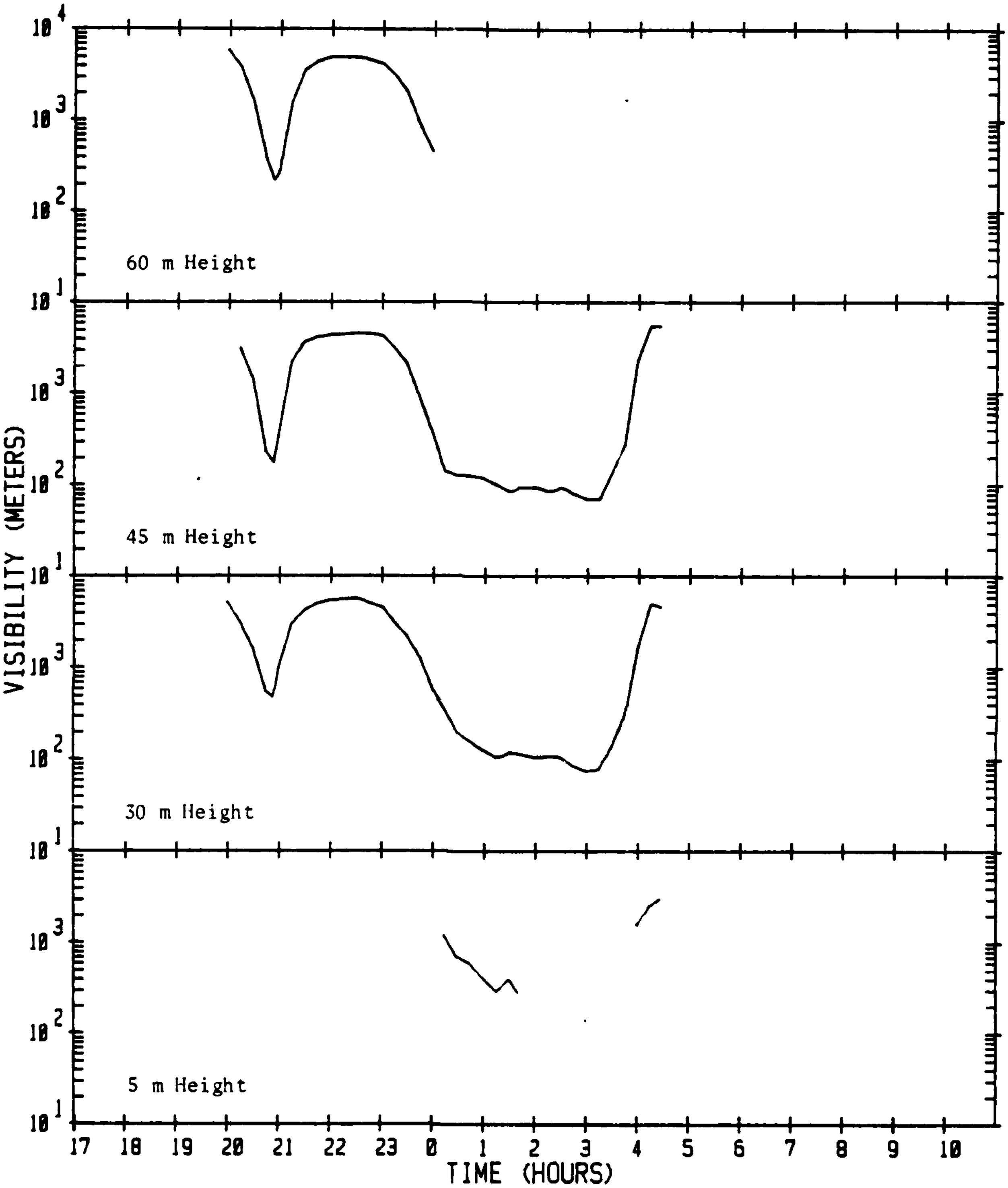

Figure 8. Visibility Records for Four Heights in the Fog of 17-18 July 1980

On two occasions, clear skys and light winds permitted the formation of very shallow ground fogs. These fogs occurred during the hours ~0200-0600 EDT on 5 July and 2300-0200 EDT on 13-14 July. Both fogs were ~1-2 m in depth, were patchy, and appeared to be most dense and persistent in the tall grass (~0.8-0.9 m high) which covered most of the field site. Fog was almost non-existent over mowed areas, roads and abandoned ramps.

- Fog Droplet Size Data

The primary objective of Calspan's participation in AFGL's fog study at Otis was the acquisition of droplet size spectra data with Calspan's Droplet Sampler for comparison with data obtained with an AFGL-operated PMS Forward Scattering Spectrometer Probe (FSSP-100). To this end, Calspan data were acquired at intervals of from 3 to 40 minutes in four of the six advection fogs which occurred during the field study. (Data were not obtained in the fog of 1-2 July because the fog was never very dense at the surface (see Figure 3) nor in the fog of 17-18 July due to instrument problems.) A total of 104 usable drop samples was obtained at the 5 m height for comparison with AFGL data; 16 additional samples were acquired at the 44 m height on the tower.

By mutual agreement, 41 of Calspan's droplet samples were reduced and analyzed, 33 from the 5 m height and 8 from the 44 m height. Raw droplet size distributions, corrected for collection efficiency, were combined with extinction data via Eq. 1 to provide estimates of droplet concentration and liquid water content. Results of these analyses and other droplet distribution parameters are tabulated in Table 2. Plots of the droplet size spectra are provided in Appendix B. Averaged surface-level (5 m ht.) data from Table 2, excluding data obtained when visibility was >400 m, are compared in Table 3 to those of previous fogs observed by Calspan.

During the early portion of the field study, a Royco Optical Particle Counter was also operated to provide measurements of particle (and droplet*) concentrations. Ten-minute-average data obtained with this device are shown at hourly intervals, where available, in Table 4. Instrument malfunction after

*We believe that lack of isokinetic sampling conditions prevent adequate sampling of fog droplets with this device; however, the data are presented here for completeness.

Table 2. Fog Microphysics at Selected Times in Fogs at Otis AFB

5m Height							44 m Height						
TIME (EDT)	MODE RADIUS (μm)	MEAN RADIUS (μm)	DROP RAD. SIZE RANGE (μm)	DROP CONC. (#/cm^3)	LWC (g/m^3)	VISIBILITY (m)	TIME (EDT)	MODE RADIUS (μm)	MEAN RADIUS (μm)	DROP RAD. SIZE RANGE (μm)	DROP CONC. (#/cm^3)	LWC (g/m^3)	VISIBILITY (m)
2-3 July 1980													
0342	4.5	6.7	2-21	29.0	.063	310							
0425	4.5	7.0	2-23	41.2	.119	190							
0526	4.5-6.5	8.1	2-21	30.9	.113	200							
3-4 July 1980													
2108	5.5-8.5	8.8	3-21	50.0	.210	110							
2200	7.5	7.9	2-19	13.6	.039	510	2159	2.5	3.6	1-21	183.5	.094	150
2221	4.5	7.0	2-20	17.3	.045	460	2227	3.0	4.0	1-17	156.0	.094	150
2329	5.5	6.8	3-17	35.6	.068	260							
0051	4.5	6.1	3-15	47.7	.066	240							
0150	5.0	7.3	2-18	38.9	.097	200							
0331	5.5	7.3	2-22	49.7	.143	150							
0455	6.0	7.9	3-20	45.3	.137	150							
10-11 July 1980													
2040	3.0+8.0	5.3	2-25	13.3	.023	900							
2145	3.5+8.5	5.4	2-22	27.2	.049	430	2146	3.5	4.7	2-18	211.0	.193	82
2207	3.5+7.5	6.9	1-31	32.5	.117	220	2215	3.5	5.1	2-23	57.2	.075	250
2234	2.5+6.0	4.8	1-23	70.9	.092	205							
2306	6.0	7.2	2-22	42.2	.129	175							
0004	6.5	8.2	2-28	28.2	.106	220							
0052	6.0-11.0	9.3	2-24	14.9	.078	320							
0142	8.0	9.6	3-24	7.5	.043	600							
0254	4.0-7.0	7.7	2-20	43.9	.131	160							
0319	6.0	7.7	2-24	67.6	.210	103							
0402	6.0	7.9	3-19	22.1	.070	300							
11-12 July 1980													
2028	4.0-8.0	7.1	2-21	6.5	.016	1250							
2223	4.0	5.7	2-22	52.7	.080	225							
2310	7.5	9.0	2-23	27.9	.139	180	2311	3.0	5.9	1-25	103.5	.206	100
2321	2.5	5.7	1-22	32.0	.075	310	2324	2.5	2.9	1-14	612.7	.143	75
2336	2.5+7.0	6.8	1-22	38.5	.104	210	2337	4.0	6.1	2-22	137.4	.235	78
0005	6.0-9.0	9.2	3-21	21.0	.099	240	2354	3.5	8.2	2-24	73.4	.365	75
0019	4.0-9.0	7.8	2-20	16.5	.052	410							
0116	5.0-10.0	9.6	2-23	27.6	.120	200							
0218	3.0-8.0	7.3	2-26	42.7	.134	170							
0317	5.0-8.0	7.1	2-22	66.0	.171	120							
0407	5.0-10.0	8.0	2-21	32.9	.105	200							

Table 3. Average Surface-Level Microphysics for Mature Stages of Dense Fogs Observed by Calspan

		Fog Type	# of Fogs	Mean Rad. (μm)	Typical Drop Size Range (Rad-μm)	Avg. Drop Conc. (cm^{-3})	Avg. LWC ($mg\ m^{-3}$)	Avg. Max. LWC ($mg\ m^{-3}$)	Avg. Min. Vsby. (m)
CONTINENTAL FOGS									
Seattle, Washington	Feb'70	Radiation	(4)	8.8	2-30	23	100	160	200-600
Otis AFB	Sep '76	Radiation	(1)	7.1	< 2-20	78	170	190	60-100
Otis AFB	Sep '76	Advect.	(1)	7.9	2-20	31	90	120	250-300
Phillipsburg, PA	Nov '65	Frontal	(2)	3.9	2-25	-	170	-	100-200
Travis AFB	Jan '73	Radiation	(13)	6.3	2-15	75	110	180	100
Elmira, NY	Aug '70	Valley	(7)	8.5-9.5	2-28	19	90	150	200-600
Los Angeles	Nov '71	Radiation	(2)	~1	< 2-40	>1000	170	310	40-200
Vandenberg AFB	Jul '72	Coastal	(8)	8.4	2-115	11	80	120	400-1000
MARINE FOGS AT SEA									
West Coast:	Aug '74	Convergence	(2)	10.0	2-115	20	125	230	100
	'72,'73,'74	Coastal Radiation	(6)	7-10	2-25	45	100	230	100-200
	'72,'74,'76	Stratus Lowering	(4)	7-9	2-115	10	30	70	300-1000
	'74 & '76	Shallow Patches		4.8-6.5	2-20	25	60	130	200-300
	Sep '76	Frontal	(1)	8.5	2-25	17	60	95	200-600
Nova Scotia:	Aug '75	Shallow Cold Water Adv	(1)	5.2	2-15	45	30	150	100
		Deep, Dense	(6)	7.5	2-115	75	230	320	80-150
		Deep, Moderate	(4)	5.6	2-115	45	55	85	200-600
Otis AFB:	Jul'80	Advection	(4)	7.5	2-22	40	110	150	150-300

Table 4. Particle Concentration Data at Sizes greater than the Indicated Diameter as Measured by a Royco OPC During Fog Episodes at Otis AFB, July 1980

DATE	TIME	>0.3 μm	>0.5 μm	>1.2 μm	>3.0 μm	>5.0 μm
1 Jul	1700 EDT	63.5/cm^{-3}	23.3/cm^{-3}	11.8/cm^{-3}	3.46/cm^{-3}	0.0004/cm^{-3}
	1800	58.1	19.7	9.4	2.79	0.0018
	1900	59.5	24.9	13.7	4.77	0
	2000	85.0	44.0	28.2	12.70	0.0004
	2100	112.1	49.7	29.4	11.10	0.049
	2200	202.5	98.1	59.5	22.9	0.049
	2300	244.6	133.2	88.9	39.7	0.067
2 Jul	0000	380.8	223.3	171.8	100.4	4.269
	0100	276.7	153.2	106.2	51.7	0.304
	0200	223.0	113.0	72.3	31.3	0.074
	0300	153.6	67.2	37.3	12.7	0.014
	0400	122.9	48.5	25.7	8.19	0.060
	0500	117.6	50.8	29.0	10.8	0.035
	0600	149.7	59.8	31.7	10.4	0.067
	0700	176.6	70.7	35.9	10.5	0.018
	0800	73.9	22.5	9.3	1.68	0.011
	0900	37.6	8.7	3.0	0.31	0.004
	2100	160	39.0	15.1	4.89	0.177
	2230	160	41.0	17.5	6.54	0.350
	2300	157	38.3	16.6	6.00	0.320
	2330	163	41.4	18.0	6.60	0.40
3 Jul	0000	154	39.4	17.3	6.50	0.43
	0030	165.3	44.1	20.3	7.95	0.47
	0100	162	43.1	19.5	7.49	0.53
	0130	150.1	38.1	17.1	6.69	0.40
	0200	157.6	44.0	20.7	8.39	0.64
	0230	168	48.1	23.3	9.62	0.92
	0300	205	77.3	46.6	22.2	3.09
	0330	524	334	241	121	9.9
	0610	393	215	155	85	10.2
	1945				204	8.15
	2250				157	5.98
	2310				60	4.09
4 Jul	2230			198	70	0.04
	2340			189	65	0.05
5 Jul	0150			65	36	0.04
10 Jul	2025				108	4.36
	2040				146.3	1.498
	2100				160.4	6.088
	2145				210.2	7.205
	2207				156.0	4.301
	2234				157.8	9.504
	2306				154.5	5.365
11 Jul	0004 EDT				375.0	5.512
	0052				238.0	1.498
	0100				264.8	1.848
	0142				291.4	0.187
	0200				-	22.76
	0254				-	29.43
	0300				-	35.32
	0402			324.5	135.7	1.212
	0500				294.7	0.032
	1900			317.2	124.9	0.011
	2000				253.2	0.018
	2028				195.9	0.064
	2100				276.1	0.032
	2200				-	0.742
	2223				332.9	2.297
	2300					4.618
	2310					5.230
	2321					7.572
	2336					6.141
12 Jul	0005					2.134
	0019					1.110
	0100					2.477
	0116					3.417
	0200					8.371
	0218					12.14
	0300					20.11
	0317					25.10
	0400					18.89
	0407					15.16
	0500					0.901
	0504				260.8	0.046

12 July prevented data acquisition after that date, and "overrunning channels" prevented data acquisition at smaller particle sizes in the denser fogs of 10-11 and 11-12 July.

2.3 Vertical Variation of Liquid Water Content in Fog*

Our measurements and study of fog characteristics over the past 15 years have shown that for deep fog extending to the ground, fog layers are generally well-mixed with moist adiabatic temperature profiles, except for the immediate surface and fog top regions. Assuming that moisture condenses following the moist adiabatic process and stays with an air parcel as it moves up and down in turbulent atmosphere, it seems reasonable to expect an increase in liquid water content (LWC) with height corresponding to a moist adiabatic temperature lapse.

Theoretical values of the adiabatic increase in LWC were computed for different temperatures and pressures typical of the lowest 300 meters of the atmosphere and are shown in Table 5. (The units used are g/m^3 per 20 meter interval which facilitated comparison with other* available data.) As can be seen in the table, the 20 m increase of LWC ranges from 3.4×10^{-2} g/m^3 at 0°C and 1020 mb to 5.14×10^{-2} g/m^3 at 20°C. The variation in the theoretical values is mostly with temperature; only a slight variation occurs with pressure.

These theoretical values were compared to observed liquid water content profiles from the fogs which occurred during the Otis field program. The data were obtained as 5-minute averages with the AFGL PMS probes and supplied to Calspan by AFGL personnel for this analysis. Table 6a shows the hourly averaged values of the difference in LWC between the 30 and 5 meter levels (the heights of AFGL's two Knollenberg probes) on the tower for five fogs. In general, the measured values are much larger than the theoretical values. Comparison by AFGL personnel of measured extinction coefficients (EG&G devices) with those computed from the PMS drop size distributions

---

*The theoretical portion of this work was supported by the Army Atmospheric Sciences Lab (ASL), White Sands and reported as: Rogers, C.W. and J.T. Hanley, 1980: "An Algorithm for the Increase of Liquid Water Content with Height in Fog and Water Hazes," Calspan Report 6711-M-1, 14 pp.

Table 5. Theoretical LWC Lapse Rates (per 20 m) for the Lower Atmosphere, Assuming Moist Adiabatic Temperature Lapse Rates

LWC LAPSE RATE (g/m^3 per 20 m height interval)					
	PRESSURE (mb)				
TEMP (°C)	980	990	1000	1010	1020
0	.0335	.0336	.0336	.0340	.0340
5	.0387	.0389	.0390	.0392	.0394
10	.0435	.0437	.0440	.0442	.0444
15	.0472	.0475	.0478	.0482	.0484
20	.0498	.0502	.0506	.0512	.0514

suggested that the computed extinction (β_c) values differed from the directly measured values (β_m) by the following relationship: $\beta_m = 4.2 + 0.673\ \beta_c$. Assuming liquid water varies by this same factor (a conservative assumption since the liquid water depends on the cube of the radius while extinction depends on the square of the radius), the liquid water differences in Table 6a were reduced according to the above relationship. The correction amounts to a 25% reduction in LWC at visibilities of ∿100 m and to zero correction at visibilities of ∿275 m. Corrected values are shown in Table 6b.

Air temperature at the surface in these fogs was between 15 and 20°C, hence a theoretical increase in LWC with height of ∿0.05 g/m^3 per 20 m height interval (see Table 5) would be expected. As can be seen in Table 6b, 0.05 g/m^3/20 m (±20%) was observed for ∿50% of average hourly values. However, the values for the fogs 3-4 and 10-11 July were consistently higher than the predicted value based on the assumption of moist adiabatic temperature profile.

Temperature and acoustic sounder records were available for the fog of 3-4 July. Inspection of these data indicated that a temperature inversion and the top of the fog were present at a height of ∿45 m, and thus the 30 m

Table 6. Hourly Average Difference in Liquid Water Content Between the 30 m and 5 m Heights in the Otis Fogs of July 1980, Normalized to a 20 m Height Interval

LWC LAPSE RATE (g/m^3 per 20 m height interval)

DATE	Average Hourly Data, Hour (EDT) Ending 22	23	00	01	02	03	04	05	06
				a. Raw Values					
2-3 July	-	-	-	-	-	-	.040	.072	.080
3-4 July	.096	.104	.102	.120	.128	.120	.120	.112	-
10-11 July	.120	.096	.112	.088	.088	.120	.088	.072	-
11-12 July	.048	.096	.080	.080	.112	.128	.120	.056	-
17-18 July	-	-	-	.040	.080	.072	.072	-	-
				b. Corrected Values					
2-3 July	-	-	-	-	-	-	.03	.06	.06
3-4 July	.07	.08	.08	.08	.09	.08	.08	.08	-
10-11 July	.09	.07	.07	.06	.06	.08	.07	.05	-
11-12 July	.03	.06	.04	.05	.07	.08	.08	.05	-
17-18 July	-	-	-	.04	.05	.04	.04	-	-

measurement level was near the height of the maximum in LWC. Accordingly, the LWC differences between the two measurement levels were probably not taken through an adiabatic layer but rather through a layer in which the top sampling level was influenced by the LWC maximum. Temperature and acoustic sounder records were not available for 10-11 July, but the synoptic situation was similar (a weak surface ridge conducive to a low level inversion) suggesting that the larger observed values of LWC increase with height might also be related to sampling in the region of maximum LWC rather than in the adiabatic layer beneath the maximum.

More rigorous analyses of these data are required to carry this interpretation any further.

2.4 The Influence of Vegetation on Dew and Fog Water Exchange at the Surface

The importance of moisture exchange at the surface to the life cycle of fog has been recognized since early investigations, e.g., Taylor (1917)*. Yet, little attention has been given to investigation of specific exchange processes as they occur through the fog life cycle. In our study of valley fog (Pilie et al, 1975), extensive measurements were made of dew deposition from six hours before fog formation through fog dissipation. First attempts to incorporate dew-related processes into fog models were also made at that time. The study successfully demonstrated the importance of dew in the development of the dew point inversion, the consequent retardation of fog formation and the importance of dew evaporation in maintaining saturation with post-sunrise heating, thus retarding fog dissipation.

The dewplate technique was used for these measurements; potential errors due to imperfect simulation of the grassy surface with a flat plate were recognized, and uncertainty as to the source of moisture deposited as dew (i.e., transported down from the air--dewfall; or up after evaporation from the ground--distillation**) was discussed.

---

*Taylor, G.I., 1917: "The Formation of Fog and Mist," Quart. J. Roy. Met. Soc., 43, pp 241-268.

**To provide supporting data for dew deposition measurements at Otis as well as to gain some insight into heat exchange processes at the surface, temperature profiles were measured in the lowest 90 cm of the air (i.e., within the height envelope of the meadow grass at Otis) and in the upper 6 cm of the soil beneath. The tallest grass in the area of the temperature probes was ∿90 cm. Using Omega thermistor probes, an amplifier and a signal scanner, temperature measurements were obtained at ∿15 min intervals continuously during the program. Air temperatures were measured at heights of 10, 40 and 90 cm above the ground. Soil temperatures were measured at the surface and at depths of 2 and 6 cm below the surface. The surface probe was placed directly on the soil surface, beneath the mantle of fallen grass and exposed roots, and was not visible from above. Temperature records for the period ∿1700 - ∿0900 EDT from four selected fog nights are provided in Appendix C.

Lala et al (1975)* expanded the early modeling efforts and tested the effects of dew on fog in numerical experiments. They clearly demonstrated the retardation of radiation fog formation by dew deposition, and their calculations suggested that substantial portions of measured dew must originate from soil moisture evaporation.

In their experimental study of the relationship of dew to radiation fog, Pickering and Jiusto (1978)** confirmed earlier conclusions that dew deposition retards fog formation and provided the first quantitative information on the relative importance of dewfall and distillation. By comparing measured dew deposition with K-theory calculations of moisture transport and with tower measurements of the formation of the dewpoint inversion, they concluded that approximately 60% of the collected dew resulted from distillation.

Pickering and Jiusto used both the dewplate and the Hiltner-type dew meter (Nagel 1962)*** for measurement of dew accumulation and expressed preference for the dewplate technique. Their measurements indicate very substantial and, on occasion, accelerated dew deposition after fog formation, which is contrary to our observations at Elmira. The differences could be associated with different characteristics of the fog or of the dew collector. In the Elmira measurements, the fog was sufficiently deep to effectively reduce nocturnal radiation divergence at the surface to zero. Whether or not this was true in the Albany measurements is uncertain. Another possibility is that Hiltner dew meter, which consists of a nylon fiber gauze suspended 10 cm above the surface, is an effective collector of fog droplets and thus collected fog liquid water rather than deposition of moisture by direct condensation on the collection surface.

---

* Lala, G.G., E. Mandel and J.E. Jiusto, 1975: "A Numerical Evaluation of Radiation Fog Variables," J. Atm. Sci., 32, pp 720-728.

** Pickering, K.E. and J.E. Jiusto, 1978: "Observations of the Relationship Between Dew and Radiation Fog," JGR, 83, No. C5, pp 2430-2436.

*** Nagel, J.F., 1962: "On the Measurement of Dew," Arch. Met. Geoph., 11, pp 403-423.

In summary, the importance of moisture exchange processes at the surface is now well established, but different measuring techniques yield different results which are not easily interpreted. Confusion often prevails. To elucidate some of the problems, Calspan initiated an internally-supported study in which we are comparing conventional dewplate measurements with measurements made with "dewplates" that simulate the natural environment in as much detail as is possible. The initial opportunity to make these comparisons occurred during the Otis field program, so that results to date are included in this report. The two dewplates used at Otis are pictured on their scales in Figure 9.

The conventional dewplate (shown at the right in Figure 9) consisted of a 500 cm^2 aluminum plate painted with flat-black "Rustoleum" (emissivity = 0.92) to simulate as nearly as possible the radiative characteristics of moist, green vegetation. This same device, with a freshly prepared surface was used to obtain the dew deposition measurements previously reported by Calspan (Pilié et al, 1972, 1975; and Mack and Pilié, 1973*).

A simulated meadow was produced by quantitatively removing the grass from 500 cm^2 of natural meadow, drying in fine sand to preserve the natural shape of each blade, and reassembling between strips of polyurethane foam to cover the 500 cm^2 dewplate. Quantitative removal of the meadow grass was accomplished by threading two strips of heavy cloth tape through the grass at the soil surface. The two tape strips, threaded carefully one inch apart with adhesive facing inward, were pressed together to trap all grass between them. The grass was then clipped from the roots with shears. After reassembly between polyfoam strips, the grass and polyfoam were painted with the same black paint as the dewplate. The simulated-meadow dewplate is shown at the left in Figure 9.

*Mack, E.J. and R.J. Pilié, 1973: "The Microstructure of Radiation Fog at Travis Air Force Base, Calspan Report No. CJ-5076-M-2, 73 pp.

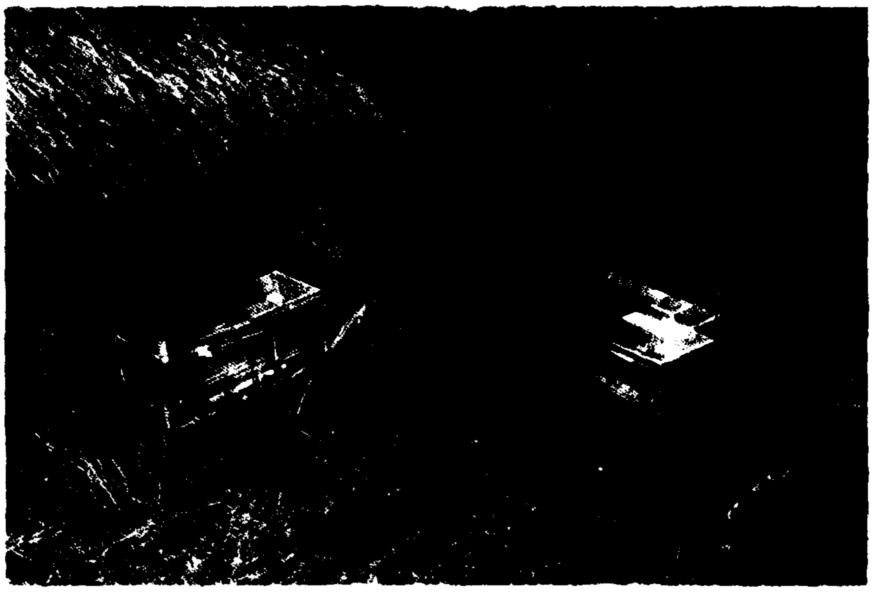

Figure 9. Photograph of Two Versions of Calspan's Dewplate Employed at Otis AFB, July 1980

The two scales bearing the dew collectors were placed in the meadow at the Otis field site ∿30 m from the main instrument tower where natural grass height was very nearly the same as the height of grass in the simulated meadow. Dew weight was usually measured hourly between 2000 and 0500 on each night when either dew or fog was expected. When overcast skys, precipitation or strong winds (which prevented accurate weight measurement) occurred, the observations were usually skipped. As a result of these procedures, conventional dewplate data were obtained on 8 nights. Comparative measurements were obtained on seven of those nights including five during which there was no fog, one during which persistent ground fog existed and one during which advection fog persisted.

During the no-fog situations at Otis, the rate of dew deposition on the simulated meadow exceeded that on the flat dewplate by a factor of 1.9 ± 0.23. During these measurements, it was realized that the thick polyfoam pad could have an effect on the amount of dew collected, so that the factor of 1.9 would not be attributable solely to the grass. Upon return to Buffalo, the measurements were continued with a painted foam pad resting on the flat dewplate. The only other difference between the Buffalo and Otis dew-collector set-up was then the presence of the meadow grass in the Otis measurements. Data obtained to date indicate that the entire factor of 1.9 was due to the foam; i.e., to within the accuracy of the measurements, the dewplate with the painted foam slab collected the same amount of dew through the night as did the dewplate with the simulated meadow employed at Otis. Apparently, the greater surface area of the polyfoam slab was responsible for the increased dew collection. While this result was completely different from what was anticipated, we considered it to be highly significant in that it lends further quantitative credence to the use of the dewplate for field measurements of dew deposition.

During the deep advection fog of 10-11 July at Otis, the dewplate collected moisture at a rate of 13 $g/m^2/hr$ before ∿2300 and 5 $g/m^2/hr$ after 2300. In the same period, water collections by the simulated meadow were respectively 59 $g/m^2/hr$ and 37 $g/m^2/hr$. The fog was sufficiently thick through this period to produce radiative equilibrium at the surface and prevent dew deposition by direct condensation. The collection of moisture was due to droplet impaction. The relative amount of water collected on the meadow grass and on the foam pad has not yet been determined. Similarly, measurements made during the thin ground fog also indicate substantial water collection by droplet impaction. We are awaiting the occurrence of fog at our Buffalo site so that clarifying measurements can be made.

In view of the above findings, only data obtained with the conventional dewplate have been used to characterize dew deposition at Otis. Data from eight nights are presented in Figure 10. (Shallow ground fog occurred on the night of 4-5 July; deep advection fog occurred on the night of 10-11 July; and dense hazes occurred on the nights of 8-9, 9-10 and 14-15 July.) Several interesting features are notable. In all cases, deposition rate was very close to constant for long periods of time. On three of the eight nights (i.e., 4-5, 10-11 and 14-15 July), however, the rate changed significantly at about midnight and then persisted at the new rate until dawn. We suspect these changes resulted from changes in the radiative properties of the lower atmosphere and/or precipitation on the dewplates, both phenomena related to the fog or dense haze present on those evenings. Note, for example, that the change in dew deposition rate on the night of 4-5 July occurred at ~0030 EDT, the time at which the ground fog of that night initially formed (see Appendix A).

The mean deposition rate at Otis was approximately 23 $g/m^2/hr$, which is consistent with observations made elsewhere. The range of observed deposition rates, 12 to 55 $g/m^2/hr$, is greater than any observed on our previous trips, but well within the range observed by other investigators (Geiger, 1965). We suspect that the greater overall variability, perhaps including the change in deposition rate on a given night, is associated with the complex geography and resulting variation in airmass moisture content of the coastal Cape Cod area compared to valleys and inland planes where our previous measurements were made.

As indicated earlier, impaction and collection on the simulated meadow in the one fog for which data are available was substantially greater than the above-reported measurement from the dewplate. While sufficient data

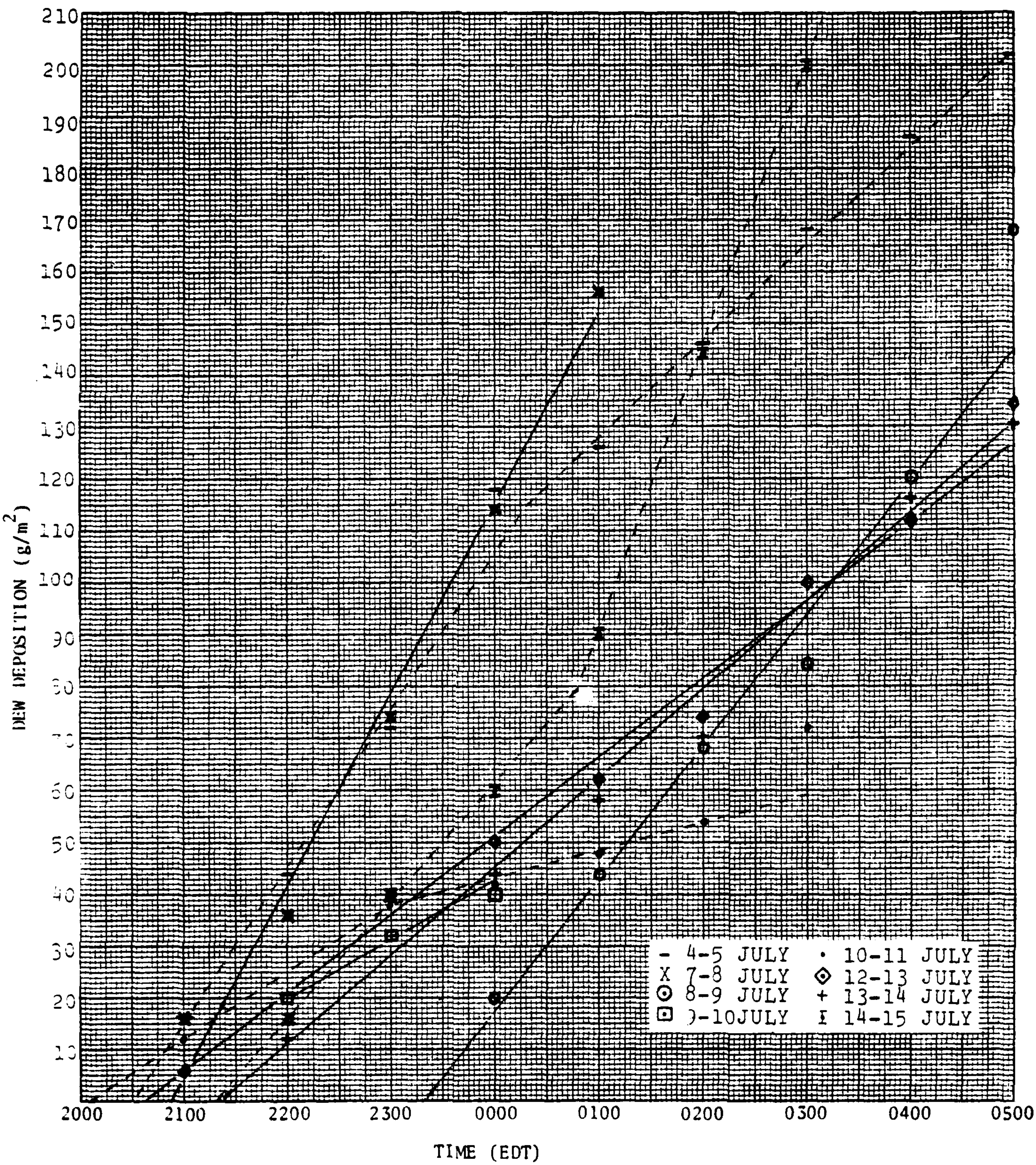

Figure 10. Dew Deposition as a Function of Time at Otis AFB, July 1980

have not yet been collected to quantify the influence of vegetation (in this case meadow grass) on the in-fog near-surface moisture budget (i.e., collection of fog droplets), the observations show that the rate of fog water collection by meadow grass in <u>dense</u> fogs can be substantially greater than the rate of dew deposition. The influence of this surface-collection of fog water on low-level fog characteristics and, potentially, on the retarding of fog dissipation after sunrise deserves further study.

2.5 Aerosol Characteristics at Otis AFB, July 1980

During the July 1980 field study at Otis AFB, measurements were obtained to characterize pre-fog ambient aerosols. These efforts included measurements of aerosol size spectra and CCN concentrations and collection of aerosol samples (via cascade impactor) for elemental composition analysis. Aerosol size spectra were measured with TSI Electrical Aerosol Analyzer and a Royco OPC at approximate hourly intervals; early evening aerosol size spectra data (one size distribution for each night of the field study) are provided in Appendix D. CCN and aerosol composition data are discussed below.

- CCN

CCN measurements were generally obtained twice each night of the field study: in the early evening at ∿2100 EDT and in the early morning, typically at ∿0400 EDT. The instrumentation and methodology used in acquiring CCN data are discussed in Section 2.1. The time histories of CCN concentrations at 0.2, 0.5 and 1.0% supersaturation (S) during the field study are shown in Figure 11. The plot shows that fluctuations of CCN during the field study were, at times, as great as an order of magnitude (over a period of 24-48 hours) and that these fluctuations were generally coincident, if not of the same magnitude, at the three supersaturations.

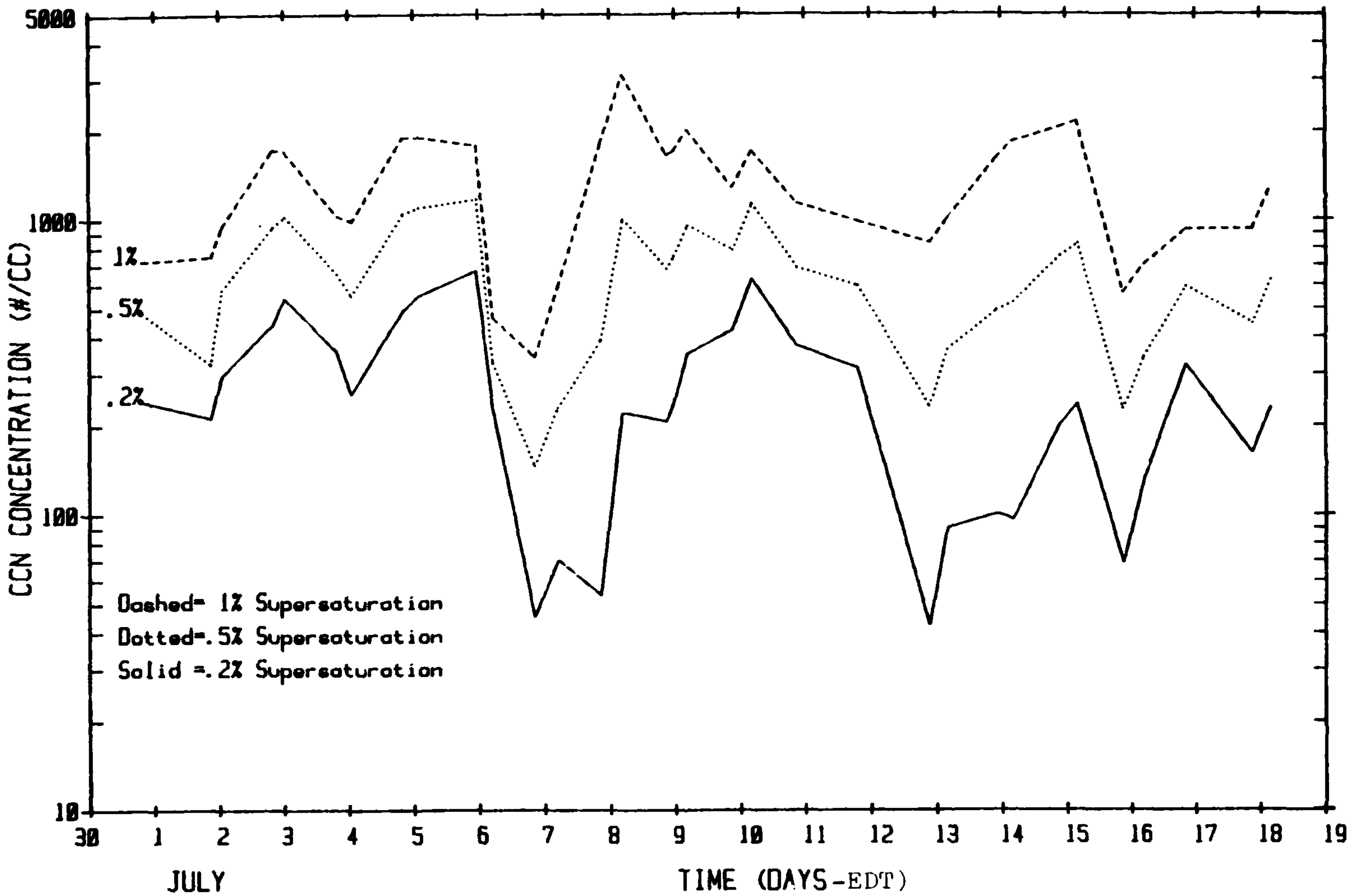

Figure 11. CCN Concentration at Indicated Supersaturations as a Function of Time at Otis AFB, 30 June to 18 July 1980

Inspection of plots of the individual activity spectra (presented in Appendix E) revealed that the spectra fell in four distinct groupings, corresponding to four time intervals during the field study: the period 1930, 30 Jun to 2300, 5 July; 2015, 6 July to 0430, 9 July; 2100, 9 July to 1920, 11 July; and the period 2125, 12 July to 0400 (EDT), 18 July. Average CCN activity spectra for these four time intervals are plotted in Figure 12. It is immediately obvious from Figure 12 that two CCN spectra characterized the aerosol at Otis during July 1980. No meteorological explanation for these spectra is immediately apparent.

Two CCN spectra representing the data in Figure 12 from Otis are compared in Figure 13 with data obtained previously by Calspan at other, primarily maritime, locations. It is seen that the spectra and concentrations of CCN observed at Otis are similar in magnitude to those observed at some other coastal locations. Steeper slopes are generally indicative of higher proportions of smaller, less active nuclei arising from anthropogenic sources; while "flat" spectra are more typical of cleaner marine situations in which most active particles are of similar composition.

- The Elemental Composition of Individual Particles

During the Otis field program, aerosol samples were collected at a height of $\sim$1 m via a Casella cascade impactor, and the samples were returned to Calspan for analysis via scanning electron microscopy (SEM) and elemental energy dispersive x-ray analysis (EDXA). The combination of these two techniques allowed (1) visualization of the impacted particle where size measurements could be obtained and (2) determination of elemental composition of particles with specific identification of elements from sodium (atomic number 11) and greater in atomic number. The analysis equipment, procedures and output are discussed in detail elsewhere (e.g., Mack et al, 1978*).

*Mack, E.J., R.J. Anderson, C.K. Akers, and T.A. Niziol, 1978: "Aerosol Characteristics of the Marine Boundary Layer of the North Atlantic and Mediterranean During May-June 1977," Calspan Report 6232-M-1, 215 pp.

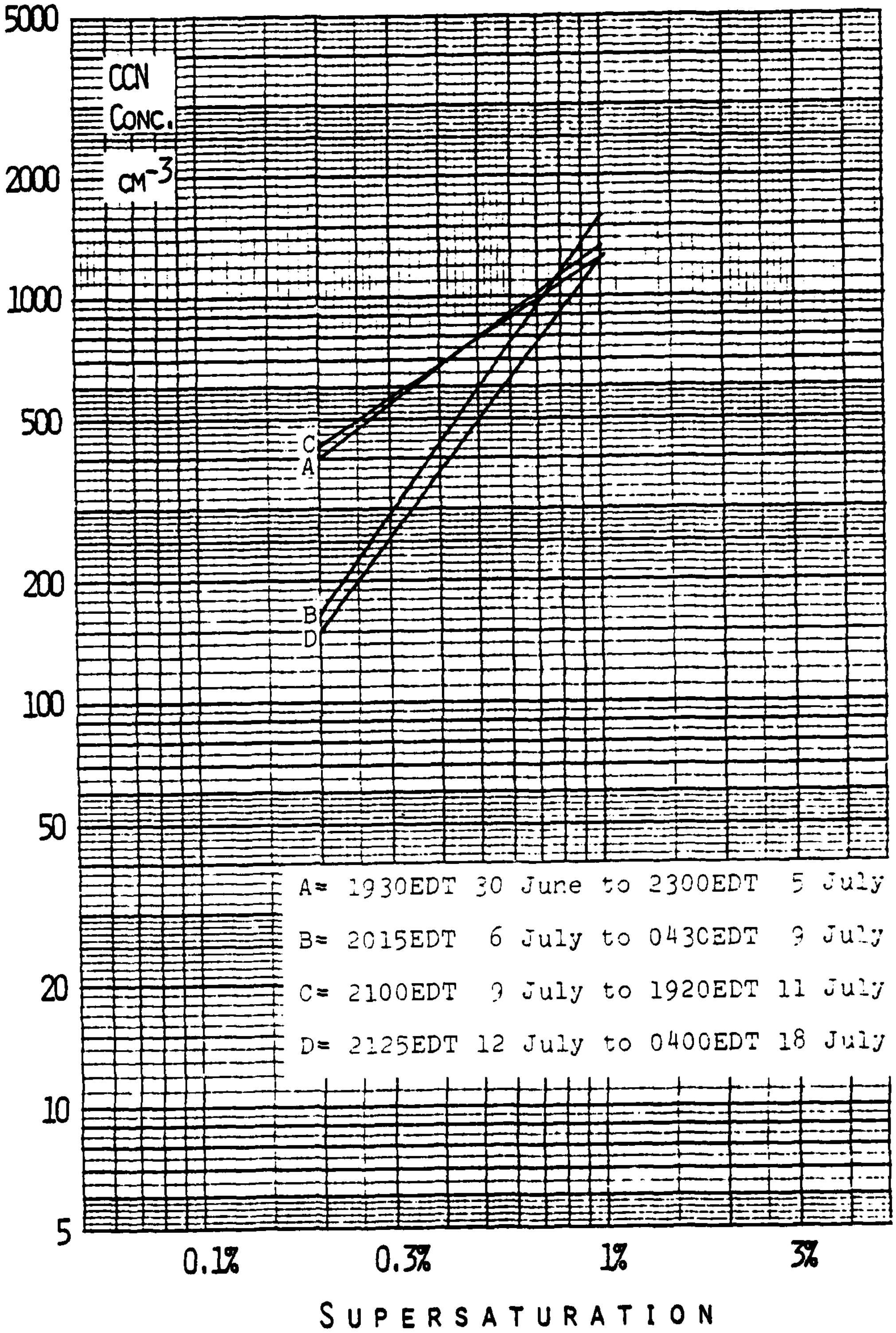

Figure 12. Average CCN Activity Spectra for Four Time Periods During the July 1980 Study at Otis AFB

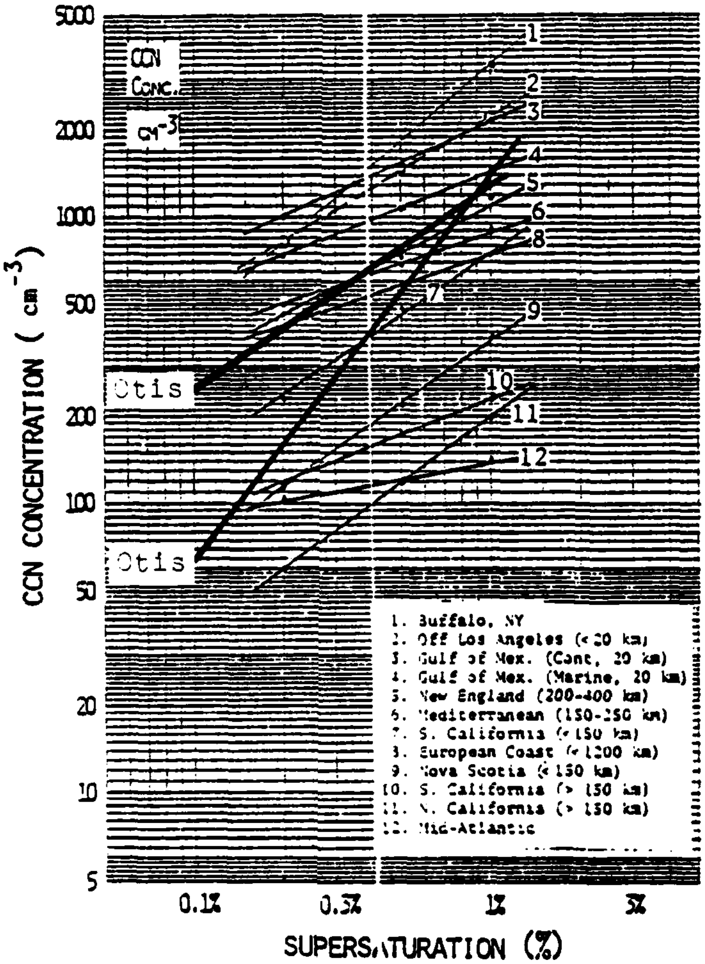

Figure 13. Average CCN Activity Spectra at Otis AFB (July 1980) Compared with Data Obtained at Other Locations

Samples were acquired over 10 min sampling periods on eight nights during the field program. For each sample, ∿50 particles were selected objectively from 50 μm wide swaths and examined using SEM and EDXA techniques. Of the 360 particles examined, a wide variety of particle shapes and compositions were seen; the particles were either rectangular, globular, or irregular in shape. No cubic NaCl particles were found. In most cases, the particles were not perfect crystals, but a few readily identifiable shapes (such as fly ash, sulfuric acid particles, etc.) were seen.

After length and width dimensions were measured, the elemental composition of each individual particle was determined using energy-dispersive x-ray analysis. As was the case for our previous studies of natural aerosol composition, it was found that individual particles could be grouped into five categories according to total elemental composition:

(1) those with atomic numbers lower than Na;
(2) NaCl only--sea salt;
(3) NaCl with minor amounts of other inorganic salts;
(4) inorganic salts without NaCl;
(5) and Si containing compounds.

The distribution of the examined particles, in percentage, as a function of composition category for each of the samples is shown in Table 7. Also shown in the table are the date and time of each sample, wind direction, and the number of particles counted in the analysis. Immediately evident from these data is that relatively few NaCl (sea salt) particles and particles of mixed NaCl and other salts composition were observed, except for the samples of 16 and 17 July, and that a dominant fraction of the collected aerosols contained silicates. The data from Otis were averaged and are compared in Table 8 with data obtained by Calspan at other maritime locations. Compared to the other maritime locations, and aerosol sampled at Otis, on the average, comprised considerably greater numbers of silicates and fewer particles of sea salt composition.

Table 7. Percentage of Particles in the Indicated Composition Category for Each Aerosol Sample Acquired at Otis AFB, July 1980

Date	Time (EDT)	Wind Dir/Sp (deg-mag)/(mph)	Percentage of Particles in Indicated Composition Categories					Number of Particles Counted
			<Na	NaCl	NaCl and Other Salts	Other Salts	Si	
4 July	2040	220/6	32%	0%	2%	18%	48%	50
10 July	0020	300/3	26	2	2	28	42	50
10 July	2030	180/5	20	0	4	18	58	50
11 July	1925	240/12	14	10	2	24	50	50
13 July	2330	265/4	28	0	4	12	56	50
15 July	0335	235/7	20	0	0	10	70	30
16 July	1955	240/12	20	57	13	3	7	30
17 July	2025	220/16	10	16	36	6	32	50

Table 8. The Percentage of Particles in the Size Range 0.2-10.0 μm Diameter as Functions of Composition and Sampling Location

		< Na* (%)	NaCl (%)	Mixed: NaCl and Other Salts (%)	Other Salts Without NaCl (%)	Si (%)	Total Particulates Counted
Coast of Portugal (within 1200 km)	May 77	33	25	17	13	12	200
Mediterranean	Jun 77	17	22	8	44	9	400
New England Coast (within 300 km)	May 77	2	81	11	3	2	150
Gulf of Mexico (20 km offshore)							
Marine	Nov 78	14	80	1	2	3	239
Continental	Nov 78	27	25	3	34	11	280
Coast of South California (within 150 km)	May 78	39	15	1	24	21	1350
Mid-Atlantic	May 77	12	68	10	8	2	300
Otis AFB (Cape Cod)	Jul 80	21	9	8	16	46	360

*Particles composed exclusively of elements with atomic numbers lower than Na

(1) Chemical Species Composed of Elements of Atomic Number Less than Na

As shown in Tables 7 and 8, approximately 20% of the aerosols observed at Otis were found in this composition category. There are ten elements of atomic number less than sodium which could make-up the particulates containing only those elements. However, only four of those have a high probability of being found in the atmosphere: H, N, C, O. There is a good probability that these particles were organic in nature and of continental/anthropogenic origin, their sources being either combustion products, photochemical processes, or natural continental material.

If the particles are inorganic, then a cation and an anion combination must be formed from those four elements. The only logical cation formed from H, N, C and O in the atmosphere as particulate is the ammonium ion (NH_4^+). There are several combinations of C, N, O and H which may form inorganic anions, the most likely of which are NO_3^- and CO_3^{--}. It is unlikely that ammonium nitrate was the primary aerosol, since it sublimes under the evacuated conditions of the SEM and would not have been detected as a particle. Ammonium carbonate is not commonly found in the atmosphere. The lack of available inorganic ions, therefore, leaves the strong probability that these aerosols were organic material.

(2) Particles Composed Solely of NaCl

A second categorization of the aerosols observed during the field study were those composed solely of NaCl. In general, these particles were globular and not cubic in shape. These particles are thought to be either sea salt aerosols whose other major constituents are at least an order of magnitude lower in concentration or organics which did not show up in the x-ray analyses. Contrary to expectations, NaCl aerosols were observed in substantial numbers on only three of the eight nights, i.e., 11, 16 and 17 July, indicating that the Otis airmasses were not of primary marine character even though winds were predominantly from the S to SW. Apparently, a tremendous continental influence overwhelmed any inputs to the aerosol loading from the sea.

(3) Mixed Aerosols Composed of NaCl and Other Inorganic Salts

The third chemical classification is that of aerosols composed primarily of NaCl with a small amount of co-precipitated inorganic salts presumably of continental origin. The relative amount of inorganic salt that was observed co-precipitated with NaCl was always less than 10 percent of the amount of NaCl present, based on the Cl x-ray peak. On our previous studies, the occurrence of this aerosol type was attributed to scavenging/coagulation processes during long residence times over the ocean. As shown in Table 7, this type of particle only occurred in substantial numbers on the nights of 16 and 17 July, suggesting that the observed continental aerosols had relatively short residence times over the ocean.

(4) Aerosols Composed of Non-NaCl Inorganic Salts

The fourth chemical classification of aerosols observed during the study was that of inorganic salts which did not contain NaCl. These particles were found to comprise $\sim$15% of the aerosol population, averaged over the eight nights for which data are available. Table 9 illustrates the number of particles of each elemental composition found in each of the specific samples. The data exhibit no trends with respect to time and show that this group of aerosols consisted primarily of particles which contained only S, P or Ca or a combination of Na and S or Ca and S. The aerosols from Otis in this grouping differ substantially and are of much greater variety than those previously observed in other maritime locations. Of the 26 different elemental combinations observed, 19 were observed only once.

(5) Silicate-Containing Aerosols

The final chemical composition group observed at Otis consisted of particles of continental origin which contained the element Si. In all, 52 different elemental combinations were observed containing the Si element, and these are listed in Table 10 according to the number of particles observed in each sample. The most frequently observed Si-containing particles contained the combination of Si and Al or the combination of Si-Al with combinations of

Table 9. Number of Observed Particles (0.2-10.0 μm Diameter) Composed of Non-NaCl Inorganic Salts of Indicated Mixed Elemental Composition for Each Sample Obtained at Otis AFB, July 1980

ELEMENTAL COMPOSITION	TOTAL NUMBER	4 JUL 80 2040 EDT	10 JUL 80 0020 EDT	10 JUL 80 2030 EDT	11 JUL 80 1925 EDT	13 JUL 80 2330 EDT	15 JUL 80 0335 EDT	16 JUL 80 1955 EDT	17 JUL 80 2025 EDT
S	15	5	2	-	6	2	-	-	-
S,Na	6	1	-	-	-	-	1	1	3
P	5	-	4	-	-	1	-	-	-
Ca	4	-	1	2	1	-	-	-	-
Fe	4	-	-	1	1	2	-	-	-
S,Ca	3	-	2	-	1	-	-	-	-
K	2	-	-	-	-	1	1	-	-
S,Mg	1	-	-	-	1	-	-	-	-
S,Na,K	1	-	-	-	-	-	1	-	-
S,Na,Mg	1	-	1	-	-	-	-	-	-
S,Fe	1	-	-	1	-	-	-	-	-
S,Cr	1	1	-	-	-	-	-	-	-
S,Na,Ca,K	1	-	-	-	1	-	-	-	-
S,Al,K,Ca	1	-	-	1	-	-	-	-	-
S,Al,Ni,V,Mg,Na	1	-	1	-	-	-	-	-	-
Ca,P	1	-	-	-	1	-	-	-	-
Ca,P,Mg,Na	1	-	-	1	-	-	-	-	-
Ca,Cl	1	-	-	1	-	-	-	-	-
Ca,Cl,Mg	1	-	1	-	-	-	-	-	-
Na,Mg	1	-	-	-	-	-	-	1	-
Na,Mg,K,P	1	-	1	-	-	-	-	-	-
K,P	1	-	1	-	-	-	-	-	-
Ca,Cr	1	-	-	1	-	-	-	-	-
Al,Cl,Ti	1	-	-	1	-	-	-	-	-
Ti	1	1	-	-	-	-	-	-	-
Zn	1	1	-	-	-	-	-	-	-

Table 10. Number of Observed Particles (0.2-10.0 μm Diameter) Containing Si as a Function of Additional Elemental Composition for Each Sample Obtained at Otis AFB, July 1980

ELEMENTAL COMPOSITION	TOTAL NUMBER	4 JUL 80 2040 EDT	10 JUL 80 0020 EDT	10 JUL 80 2030 EDT	11 JUL 80 1925 EDT	13 JUL 80 2330 EDT	15 JUL 80 0335 EDT	16 JUL 80 1955 EDT	17 JUL 80 2025 EDT
Si,Al	25	5	2	5	3	6	4	-	-
Si,Al,K,Fe	17	2	-	8	2	1	3	-	1
Si,Al,K,Fe,Mg	9	1	3	2	1	-	-	1	1
Si,Al,K,Fe,Ca	9	-	1	1	1	1	3	-	2
Si,Al,Fe	9	2	-	1	1	1	3	-	1
Si	7	-	1	1	3	1	-	1	-
Si,Al,Ca	7	1	-	2	2	-	1	-	1
Si,Al,K	6	1	1	-	-	3	-	-	1
Si,Al,Ca,K,Fe,Mg,Na	6	-	-	1	1	2	-	-	2
Si,Al,Ca,Fe	5	1	-	-	-	1	3	-	-
Si,Al,Ca,Na	4	1	-	1	1	1	-	-	-
Si,Al,Na	3	-	-	-	-	3	-	-	-
Si,Al,Mg,K,Na	3	-	-	1	-	1	-	-	1
Si,Al,Cl,Fe	3	-	1	1	-	-	-	-	1
Si,S	3	2	1	-	-	-	-	-	-
Si,Al,S,K,Fe	3	-	3	-	-	-	-	-	-
Si,Ca	2	1	-	-	1	-	-	-	-
Si,K,Mg,Na	2	-	2	-	-	-	-	-	-
Si,Al,S,Ca	2	-	-	1	1	-	-	-	-
Si,Al,Na,Mg	2	-	-	-	-	2	-	-	-
Si,Al,K,Fe,Cl	2	-	-	1	1	-	-	-	-
Si,Al,Fe,Na	2	1	-	-	-	-	-	-	-
Si,Al,Fe,Mg	2	-	-	-	-	1	-	-	1
Si,S,Na	2	-	1	-	-	-	-	-	1
Si,Mg,Cl,Ca	2	-	2	-	-	-	-	-	-
Si,K,Cl,Ca	2	-	-	2	-	-	-	-	-
Si,Al,Mg	1	-	-	-	1	-	-	-	-
Si,Al,Ca,K	1	1	-	-	-	-	-	-	-
Si,Al,Ti	1	1	-	-	-	-	-	-	-
Si,Al,S,Fe,Ti	1	-	-	-	1	-	-	-	-
Si,Mg,Fe,Ti	1	-	1	-	-	-	-	-	-
Si,Al,S,Fe,K,Ti	1	-	-	-	1	-	-	-	-
Si,Al,K,Fe,Ti	1	-	-	-	-	-	1	-	-
Si,Al,K,Ti	1	-	-	-	-	-	1	-	-
Si,Al,K,Ca,Fe,Mg,Ti	1	-	-	-	-	-	1	-	-
Si,Al,Fe,Ti	1	-	-	-	-	-	1	-	-
Si,Al,S,Fe,Mg	1	-	-	-	-	1	-	-	-
Si,Ca,P	1	-	-	-	-	1	-	-	-
Si,Al,S,Cl	1	1	-	-	-	-	-	-	-
Si,Al,S,K	1	-	-	-	1	-	-	-	-
Si,Mg,Fe	1	1	-	-	-	-	-	-	-
Si,Ca,Mg,Na	1	1	-	-	-	-	-	-	-
Si,Al,K,Fe,P	1	-	-	-	1	-	-	-	-
Si,Al,K,Ca,Fe,Mg	1	-	-	-	1	-	-	-	-
Si,Al,K,Ca.Fe,Na	1	-	1	-	-	-	-	-	-
Si,K	1	-	1	-	-	-	-	-	-
Si,Na	1	-	-	-	-	-	-	-	1
Si,P	1	-	-	1	-	-	-	-	-
Si,S,Fe	1	1	-	-	-	-	-	-	-
Si,Mg,Cl,Ca,Fe	1	1	-	-	-	-	-	-	-
Si,Al,Mg,S,Ca,Na,Fe	1	-	-	-	-	-	-	-	1
Si,Al,Mg,S,K,Na,Fe	1	-	-	-	-	-	-	-	1

K, Fe, Ca and Mg. The remainder of the Si-containing compounds generally were different in chemical composition at different sampling times. Of these 52 different elemental combinations, 26 were seen only once, 10 recurred twice, and 5 were sampled only three times.

APPENDIX A

Log of Meteorological Variables
Measured at Otis AFB, July 1980

		Wind		Nephelometer		Temperature			Fog Visibility at Hts:		
DATE	TIME (EDT)	Direction Deg.-Mag.	Speed (mph)	B_{scat} ($x10^{-4}m^{-1}$)	Vsby (mi)	Dry Bulb (°F)	Wet Bulb (°F)	Rel. Hum. (%)	5 m (m)	30 m (m)	60 m (m)
30 June	1700	060	5								
	1800	060	8								
	1900	060	6								
	2000	060	3								
	2100	060	4								
	2200	190	4								
	2300	060	5								
1 July	0000	010	3								
	0100	070	2.5								
	0200	325	3								
	0300	185	0								
	0400	070	2.5								
	0500	095	2.5								
	0600	205	4								
	0700	005	4								
	0800	110	2								
	1700	165	7	3.6	8.0						
	1800	170	9	3.2	9.1						
	1900	175	8	3.3	8.8						
	1930										
	2000	175	7	5.1	5.7						
	2100	190	7	8.0	3.6				>6000	>6000	>6000
	2140					61.2	60	93			
	2200	190	7	11.0					3600	2300	1800
	2230					59.9	59.5	97	1400	580	400
	2300	185	8	14.0					2800	2100	1100
	2316					60.3	59.7	97	2700	2500	1700
2 July	0000	210	7	17.0		60.1	59.7	97	2200	1050	500
	0100	180	7	16.0					1200	400	290
	0114					60.5	59.8	96	2100	1800	-
	0200	195	7	13.0		60.4	59.7	96	2500	1700	440
	0300	190	6	7.8		61.4	60.5	94	4500	>6000	4600
	0400	190	7	7.1					6000	>6000	6000
	0430					61.4	60.4	94	6000	>6000	>6000
	0500	195	6	9.1					5000	>6000	>6000
	0600	200	7	-					3100	2400	1500
	0700	205	8	8.9					3200	2500	2100
	0800	205	10	3.8	7.6				>6000	>6000	>6000
	1700	200	12	6.8	4.2						
	1800	215	7	5.2	5.6						
	1900	215	9	6.8	4.2						
	1940					67.0	64.8	89			
	2000	215	11	9.0	3.2	66.3	64.6	91			
	2100	240	12	9.3	3.1	66.4	64.7	91	>6000	>6000	>6000
	2200	250	8	10.0	2.9	67.1	65.3	91	6000	>6000	>6000
	2300	240	8	11.0	2.7	68.7	65.7	85	6000	>6000	5900
3 July	0000	255	7	14.0		67.9	66.1	91	4500	4100	4100
	0100	240	7	16.0		67.8	66.3	92	3200	3100	2900
	0200	230	5	17.0		67.3	66.1	93	3000	2800	2700
	0230	230	6						2800	2400	2100
	0300	250	3	27.0		67.1	66.1	95	1400	620	450
	0330	245	4						500	200	210
	0400	240	4	60.0		66.3	66.0	98	210	140	200
	0430	225	3						200	150	220
	0500	240	3	77.0		66.7	66.0	96	210	110	155
	0530	330	2.5						170	100	160
	0600	240	2	63.0					300	205	220
	0610					68.1	66.7	92.5			
	0630	220	2						1700	1300	625

		Wind		Nephelometer		Temperature			Fog Visibility at Hts:		
DATE	TIME (EDT)	Direction Deg.-Mag.	Speed (mph)	B_{scat} $(x10^{-4}m^{-1})$	Vsby (mi)	Dry Bulb (°F)	Wet Bulb (°F)	Rel. Hum. (%)	5 m (m)	30 m (m)	60 m (m)
3 July	0700	000	2.5	14.0					2800	2100	2400
	0800	115	2.5	8.8					4500	4000	4300
	0845								>6000	>6000	>6000
	1700	180	5	7.2	4.0						
	1800	180	7	-							
	1830	215	7								
	1900	220	8	-							
	1930	220	7						650	115	210
	1940					69.2	68.2	95			
	2000	225	6	27.0					650	140	210
	2030	240	8						1550	480	310
	2100	235	8	43.0		67.9	67.9	100	120	80	150
	2130	265	7.5						350	110	150
	2200	265	6	42.0		68.1	67.9	98	510	125	170
	2230	235	6						300	105	170
	2300	250	5	42.0		68.0	67.6	98	600	140	190
	2330	230	7						270	100	160
4 July	0000	255	5	50.0		68.0	67.5	97	310	105	190
	0030	245	8						260	95	160
	0100	255	7.5	57.0		67.7	67.3	98	260	95	160
	0130	240	9						310	130	220
	0200	255	7	67.0		67.1	66.5	97	200	87	150
	0230	250	7						240	88	155
	0300	280	5	66.0		67.8	67.2	97	290	115	170
	0330	255	7						160	90	150
	0400	250	6	79.0		67.4	67.3	99	160	80	170
	0430	260	6						210	90	160
	0500	255	7	80.0		66.8	66.4	98	155	87	200
	0530	270	7.5						190	100	200
	0600	270	6	86.0					120	65	140
	0630	260	5						300	100	190
	0700	250	7	55.0					620	205	240
	0730	275	7						1000	420	310
	0800	290	7	17.0					1500	800	500
	0830	310	5						3000	2100	2200
	0900	335	7.5						4700	4500	4500
	0930								>6000	>6000	>6000
	1700	230	7	2.5	11.7						
	1800	210	7.5	2.2	13.5						
	1900	250	6	2.7	10.7						
	1920										
	2000	220	6	5.2	5.6	70.4	65.2	76			
	2030										
	2100	190	4	6.6	4.4	62.7	60.6	89			
	2130					64.9	62.0	85			
	2200	180	6	8.3	3.5	65.1	61.7	83			
	2300	180	5	10.2	2.9	63.8	61.2	87			
5 July	0000	200	5	8.8	3.3	62.4	60.4	89	>6000	>6000	>6000
	0100	190	4	-		61.8	59.9	89	4900	>6000	>6000
	0200	230	4	25.0		60.3	59.4	94	3100	>6000	>6000
	0300	215	4	21.0		60.3	58.9	92	3800	>6000	>6000
	0400	215	3	23.0		60.8	59.6	93	4200	>6000	>6000
	0500	225	3	33.2		60.6	59.2	92	2700	>6000	>6000
	0600	220	2.5	16.6					3000	6000	>6000
	0700	195	4	6.8					5500	>6000	>6000
	0800	200	-	5.4	5.3				>6000	>6000	>6000
	1700	205	-	2.8	10.4						
	1800	215	-	5.0	5.8						
	1900	235	-	10.4	2.8						
	2000	230	-	18.4	1.6						
	2100	185	-	22.2							

DATE	TIME (EDT)	Wind Direction Deg.-Mag.	Wind Speed (mph)	Nephelometer B_{scat} $(x10^{-4}m^{-1})$	Nephelometer Vsby (mi)	Temperature Dry Bulb (°F)	Temperature Wet Bulb (°F)	Rel. Hum. (%)	Fog Visibility at Hts: 5 m (m)	Fog Visibility at Hts: 30 m (m)	Fog Visibility at Hts: 60 m (m)
5 July	2200	190	-	27.2							
	2300	200	9	26.2		67.3	66.3	95			
6 July	0000	190	7	30.8		68.2	67.1	94			
	0100	240	7.5	11.2	2.6						
	0200	250	5	5.0	5.8						
	0300	275	8	5.8	7.6	66.3	65.3	95			
	0350					66.3	65.6	96			
	0400	270	10	4.9	5.9						
	0500	270	9	4.7	6.2	66.4	65.2	94			
	0600	270	10	5.1	5.7						
	0700	300	11	3.8	7.6						
	0800	325	13	4.7	6.2						
	1700	325	18	0.75	42.0						
	1800	340	18	0.7	44.0						
	1900	345	15	0.7	44.0						
	1940										
	2000	345	11	0.75	42.0	68.3	53.7	36			
	2100	005	-	0.8	39.0	62.5	52.2	49			
	2200	010	-	0.8	39.0	59.7	50.7	52			
	2300	335	5	0.95	34.0	55.5	49.4	68			
7 July	0000	310	7	0.95	34.0	55.3	49.8	68			
	0100	325	8	0.9	35.0	56.4	50.4	65			
	0200	315	6	0.9	35.0	54.4	49.5	70			
	0300	305	7	0.95	34.0	53.8	49.5	73			
	0400	315	6	1.0	31.5	52.8	49.4	78			
	0500	305	10	1.0	31.5						
	0600	310	8	0.9	35.0						
	0700	325	11	0.95	34.0						
	0800	340	10	1.3	24.0						
	1700	255	13	1.25	24.0						
	1800	260	10	1.55	20.5						
	1900	225	6	1.55	20.5						
	2000	200	2	1.55	20.5	63.1	60.6	87			
	2100	195	4	3.0	9.7	61.2	59.4	89			
	2200	220	4	3.4	8.5	60.1	59.0	94			
	2300	245	6	2.9	10.0	61.0	59.4	92			
8 July	0000	240	6	3.8	7.6	60.9	59.8	94			
	0100	245	7	2.8	10.4	62.0	60.4	92			
	0200	245	7	3.0	9.7	62.2	60.6	92			
	0300	235	7	2.8	10.4	61.5	59.8	91			
	0400	250	7	3.1	9.3	60.4	59.2	93			
	0500	245	7	3.2	9.1	60.5	59.1	93			
	0600	230	4	2.7	10.7						
	0700	230	8	1.7	18.0						
	0800	250	12	1.7	18.0						
	1700	195	19	1.25	24.0						
	1800	200	18	1.5	21.0						
	1900	220	17	1.85	16.5						
	2000	240	17	3.0	9.7	67.0	64.7	88			
	2100	265	14	5.5	5.3	66.7	65.2	92			
	2145			9.8	3.0						
	2200	330	7	8.2	3.5	66.7	64.4	88			
	2220			3.2	9.1	64.3	62.2	90			
	2300	300	4	3.6	8.0	59.8	58.3	91			
9 July	0000	300	4	3.8	7.6	59.3	57.7	90			
	0100	285	2	4.4	6.5	59.2	57.7	91			
	0200	270	3	8.3	3.5	56.8	56.2	97			
	0230					55.8	54.7	94			
	0300	325	5	10.0	2.9	57.1	56.2	94			

DATE	TIME (EDT)	Wind: Direction Deg.-Mag.	Wind: Speed (mph)	Nephelometer: B_{scat} ($x10^{-4}m^{-1}$)	Nephelometer: Vsby (mi)	Temperature: Dry Bulb (°F)	Temperature: Wet Bulb (°F)	Rel. Hum. (%)	Fog Visibility at Hts: 5 m (m)	30 m (m)	60 m (m)
9 July	0400	290	7	14.0	2.1	60.3	59.4	94			
	0500	295	5	13.2	2.2	60.0	58.8	93			
	0600	310	7	4.6	6.3						
	0700	320	4	2.6	11.3						
	0800	340	7	2.3	12.3						
	1700	255	14	2.0	15.0						
	1800	250	16	2.0	15.0						
	1900	250	13	2.8	10.4						
	2000	245	12	3.8	7.6	67.6	63.4	80			
	2100	250	8	4.5	6.4	67.1	63.4	80			
	2130										
	2200	245	5	5.8	5.0	66.3	63.7	87			
	2300	255	7	6.4	4.5	66.3	64.1	90			
10 July	0000	225	6	8.7	3.3	65.2	63.6	92			
	0100	260	5	7.1	4.1	66.6	64.4	89			
	0200	Calm	0	6.6	4.4	66.8	64.4	87			
	0300	235	2	7.6	3.8	65.8	64.4	92			
	0400	300	2	8.8	3.3	66.7	64.4	88			
	0500	250	4	11.0	2.7	65.6	64.4	94			
	0600	360	3	12.8	2.3						
	0700	060	7	3.4	8.5						
	0800	100	7	3.0	9.7						
	1700	200	8	5.0	5.8						
	1800	190	10	4.0	7.2						
	1900	170	7	6.2	4.6				>6000	>6000	>6000
	2000	175	6	10.8		66.8	65.9	95	5800	5400	4600
	2032					66.2	65.3	95			
	2100	180	5	43.0		65.9	65.4	97.5	205	80	125
	2200	190	7	38.0					260	130	170
	2245								120	65	115
	2300	200	5	54.0					250	110	170
	2342			79.0							
11 July	0000	165	5	58.5		63.4	63.3	100	120	83	125
	0100	175	7.5	38.0		62.4	62.4	100	570	210	160
	0200	225	6	46.0		61.6	61.4	99	390	80	130
	0300	200	7	56.0		61.3	61.3	100	110	82	130
	0400	255	4	49.0		61.3	61.0	98	300	95	160
	0500	240	5	23.4		62.0	61.0	94	1800	1400	380
	0600	230	5	17.6					3000	3000	1500
	0700	215	5	13.2					2300	580	350
	0800	210	5	5.8					>6000	>6000	>6000
	1700	220	12	8.8							
	1730								5500	>6000	5500
	1800	235	14	9.2					5000	4400	3300
	1900	240	11	13.0		66.3	64.5	90	3800	3200	2800
	2000	245	15	19.0		65.5	64.4	94.5	2400	1700	550
	2100	240	15	28.0		65.2	64.3	95	1200	380	300
	2200	240	14	34.4		64.8	64.6	99	525	190	160
	2300	290	5	57.0		65.4	65.4	100	210	95	145
12 July	0000	195	13	50.5		65.5	65.4	<100	280	105	160
	0100	205	12	61.0		65.6	65.5	<100	250	105	180
	0200	215	9	68.0		66.5	66.1	97.5	180	80	140
	0300	210	8	83.0		67.0	66.5	97	130	80	140
	0400	230	7	94.0		66.6	66.5	<100	135	80	130
	0500	265	7	67.0		66.3	66.3	100	510	160	200
	0545					67.3	66.5	96	800	800	900
	0600	315	6	33.6					1650	1800	2000
	0700	005	8	9.4					5000	5700	5500
	0730								>6000	>6000	>6000
	0800	015	8	3.8	7.6						

DATE	TIME (EDT)	Wind Direction Deg.-Mag.	Wind Speed (mph)	Nephelometer B_{scat} $(x10^{-4}m^{-1})$	Nephelometer Vsby (mi)	Temperature Dry Bulb (°F)	Temperature Wet Bulb (°F)	Rel. Hum. (%)	Fog Visibility at Hts: 5 m (m)	30 m (m)	60 m (m)
12 July	1700	085	7	1.1	29.0						
	1800	160	8	1.3	24.0						
	1900	160	7.5	1.2	26.0						
	2000	145	6	1.7	18.0	63.2	58.4	74			
	2100	150	5	1.4	22.5	60.7	56.3	75.5			
	2200	175	5	1.5	21.0	59.9	56.4	81			
	2300	180	7	1.5	21.0	59.3	56.0	80			
	2330										
13 July	0000	180	3	1.6	19.5	57.0	54.4	85			
	0100	215	2	1.8	17.0	55.7	53.9	89			
	0200	220	3	2.0	15.0	55.3	53.4	88			
	0300	260	5	2.4	12.3	55.6	53.6	88			
	0400	280	3	2.6	11.3	55.4	53.3	88			
	0500	300	5	3.1	9.3						
	0600	315	5	1.9	16.0						
	0700	300	6	1.8	17.0						
	0800	305	8	1.5	21.0						
	1700	235	12	1.3	24.0						
	1800	225	8	1.3	24.0						
	1900	235	7	1.5	21.0						
	2000	235	5	1.5	21.0	68.4	63.4	76			
	2100	250	7	1.6	19.5	67.3	62.5	75			
	2200	265	4	2.6	11.3	61.8	59.9	89			
	2300	275	3	3.2	9.1						
	2315					59.3	59.2	<100			
14 July	0000	290	3	4.1	7.0	59.4	59.1	99			
	0100	300	3	4.2	6.9	59.9	59.6	98.5			
	0200	290	3	3.4	8.5	60.3	59.3	94			
	0300	305	5	2.7	10.7	59.2	58.2	94			
	0400	310	3	4.4	6.5	57.8	57.4	97			
	0445					58.2	56.6	91			
	0500	330	3	3.3	8.8						
	0600	295	4	2.4	12.3						
	0700	305	4	2.0	15.0						
	0800	305	7	1.6	19.5						
	1700			1.4	22.5						
	1800			1.5	21.0						
	1900			1.5	21.0						
	2000			2.3	12.3						
	2030	235	7			67.3	63.5	80			
	2100	255	7	3.3	8.8	66.4	63.1	85			
	2200	235	6	4.8	6.0	65.5	63.3	90			
	2300	235	5	5.1	5.7	66.3	63.7	87			
15 July	0000	210	4	7.0	4.1	63.8	61.7	90			
	0100	250	7	7.6	3.8	65.3	64.4	95			
	0200	260	7	15.0	1.9	64.3	63.9	98			
	0300	235	7	23.0		65.2	64.6	97			
	0400	235	7	17.0	1.7	65.3	64.5	96			
	0500	235	8	10.0	2.9	65.3	64.7	97			
	0600	230	8	4.0	7.2						
	0700	235	12	2.8	10.4						
	0800	245	15	2.2	13.5						
	1700	230	21	1.5	21.0						
	1800	230	18	1.4	22.5						
	1900	230	17	1.3	24.0						
	2000	235	15	1.4	22.5	70.0	63.7	68			
	2030										
	2100	220	18	1.4	22.5	70.3	63.3	68			
	2200	230	18	1.4	22.5	70.2	64.5	74			

		Wind		Nephelometer		Temperature			Fog Visibility at Hts:		
DATE	TIME (EDT)	Direction Deg.-Mag.	Speed (mph)	β_{scat} $(x10^{-4}m^{-1})$	Vsby (mi)	Dry Bulb (°F)	Wet Bulb (°F)	Rel. Hum. (%)	5 m (m)	30 m (m)	60 m (m)
15 July	2300	245	19	1.7	18.0	R A	I N				
16 July	0000	220	18	1.6	19.5	68.5	65.1	83			
	0100	230	15	1.8	17.0	60.6	68.5	90			
	0200	235	16	2.0	15.0	69.2	66.3	85			
	0300	230	16	2.6	11.3	68.3	66.7	92			
	0400	230	17	2.4	12.3	69.2	67.2	90			
	0500	235	17	2.8	10.4	69.3	67.4	90			
	0600	245	18	3.1	9.3						
	0700	240	17	3.3	8.8						
	0800	240	17	3.0	9.7						
	1700	230	16	5.9	4.9						
	1800	230	17	6.0	4.8						
	1900	220	16	7.5	3.8						
	1940					71.8	69.8	91			
	2000	245	11	10.3	2.8	70.7	69.4	93			
	2100	235	14	11.2	2.6	70.4	69.1	93.5			
	2200	190	6	13.6	2.1	70.3	69.0	94			
	2300	250	7	15.2	1.9	70.1	68.9	94			
17 July	0000	255	7	13.7	2.1	70.2	68.8	93			
	0100	235	8	10.5	2.8	70.3	68.5	90			
	0200	235	15	9.0	3.2	70.7	68.2	88			
	0300	225	15	11.0	2.7	72.7	69.4	86			
	0400	245	14	6.4	4.5						
	0500	240	15	6.2	4.6						
	0600	240	12	7.0	4.1						
	0700	255	15	7.2	4.0						
	0800	250	21	5.4	5.3						
	1700	230	18	7.8	3.7						
	1800	240	17	12.4	2.4						
	1900	230	18	8.0	3.6				-	>6000	>6000
	2000	220	15	11.0		71.5	70.1	90	-	5200	5900
	2100	220	16	18.4		71.1	70.4	97	-	1000	270
	2200	220	16	8.0		70.7	69.5	94	-	5500	5000
	2300	240	14	8.0		71.2	70.2	95	-	4500	4100
18 July	0000	250	15	14.0		69.8	69.4	98	-	570	450
	0100	250	12	23.2					425	130	-
	0115								290	105	-
	0145					68.9	68.9	100	280	115	-
	0200	250	10	30.8					-	105	-
	0300	310	6	47.0					140	75	-
	0345					68.3	68.0	97	-	300	1700
	0400	040	6	34.0		69.0	68.4	97	1600	1700	-
	0427			26.5					3100	4600	
	0500	295	4								
	0600	315	3								
	0700	350	2								
	0800	010	6								

APPENDIX B

Droplet Size Distributions
In The Fogs Of 2-3, 3-4, 10-11 and 11-12 July 1980
At Otis AFB

The droplet size spectra provided in this section correspond to the data presented in Table 2, Section 2, p.19. Each drop size distribution is annotated as follows:

T = time (EDT) of sample acquisition
R = mean radius (μm)
N = number concentration (cm^{-3})
W = liquid water content (g/m^3)
V = measured visibility (m)

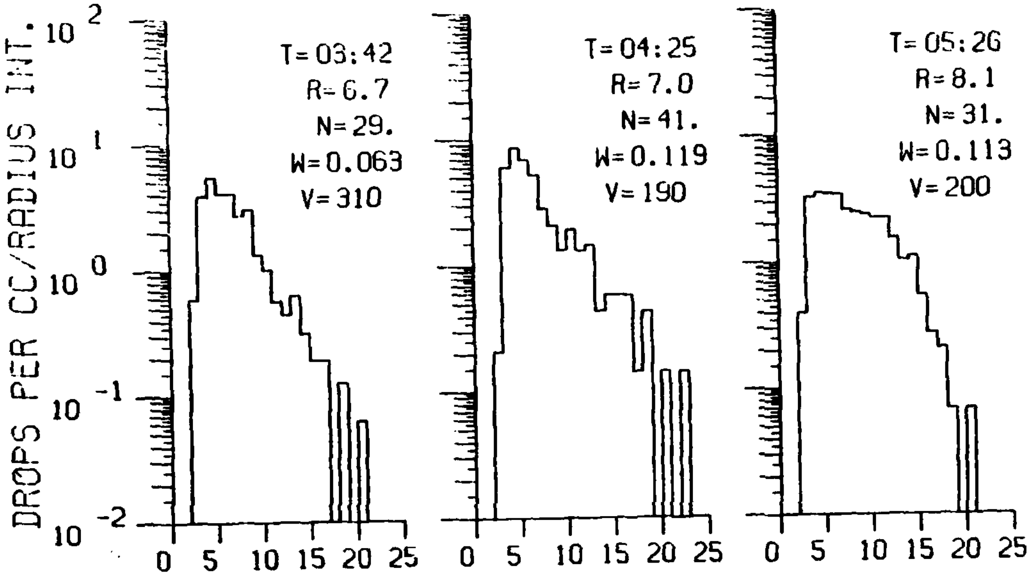

DROPS PER CC/RADIUS INT.

Figure b-1. Drop Size Spectra at Selected Times in the Fog of 2-3 July 1980

5 Meter Height

RADIUS (MICRONS)

2-3 JUL1980

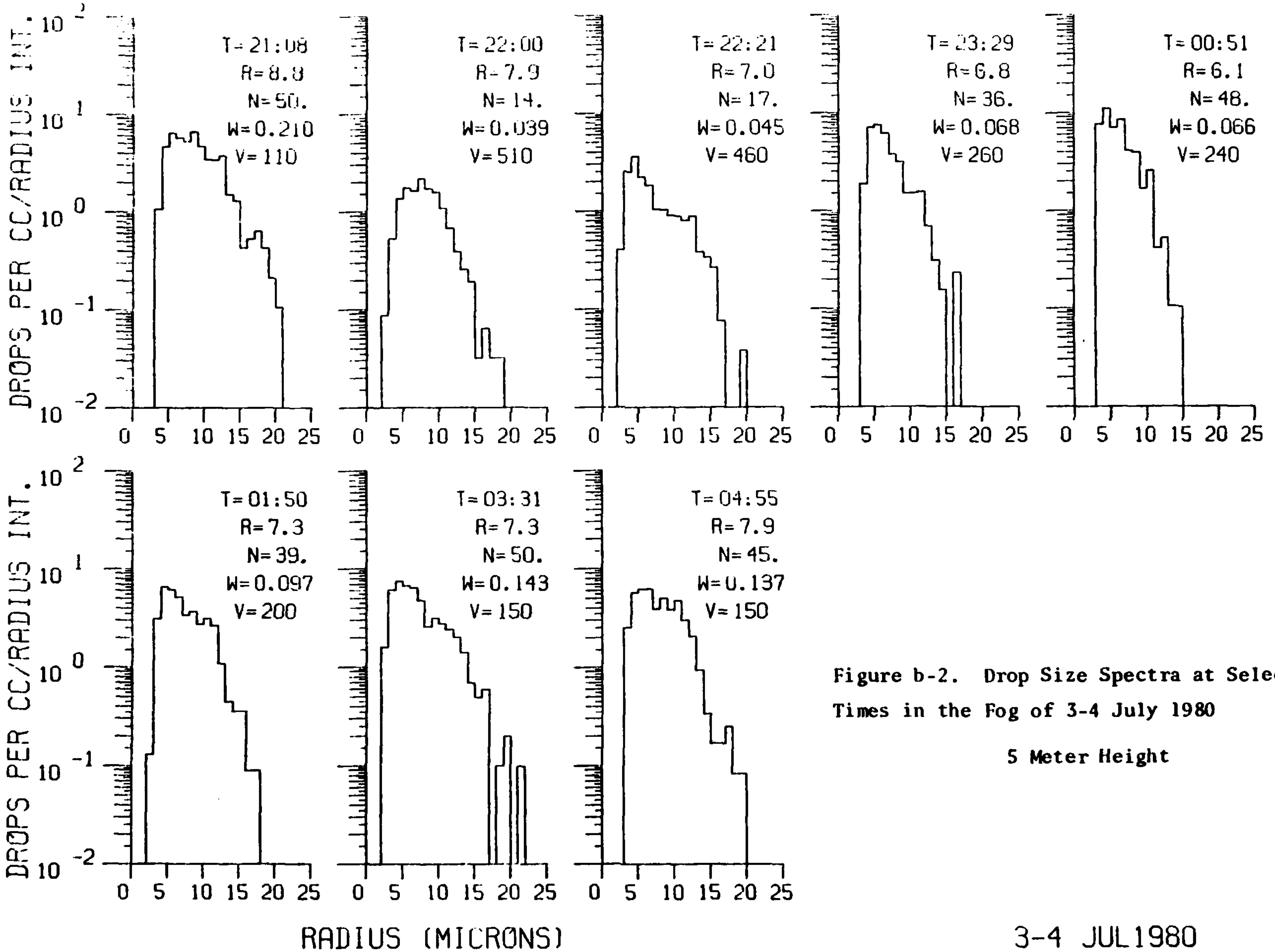

Figure b-2. Drop Size Spectra at Selected Times in the Fog of 3-4 July 1980

5 Meter Height

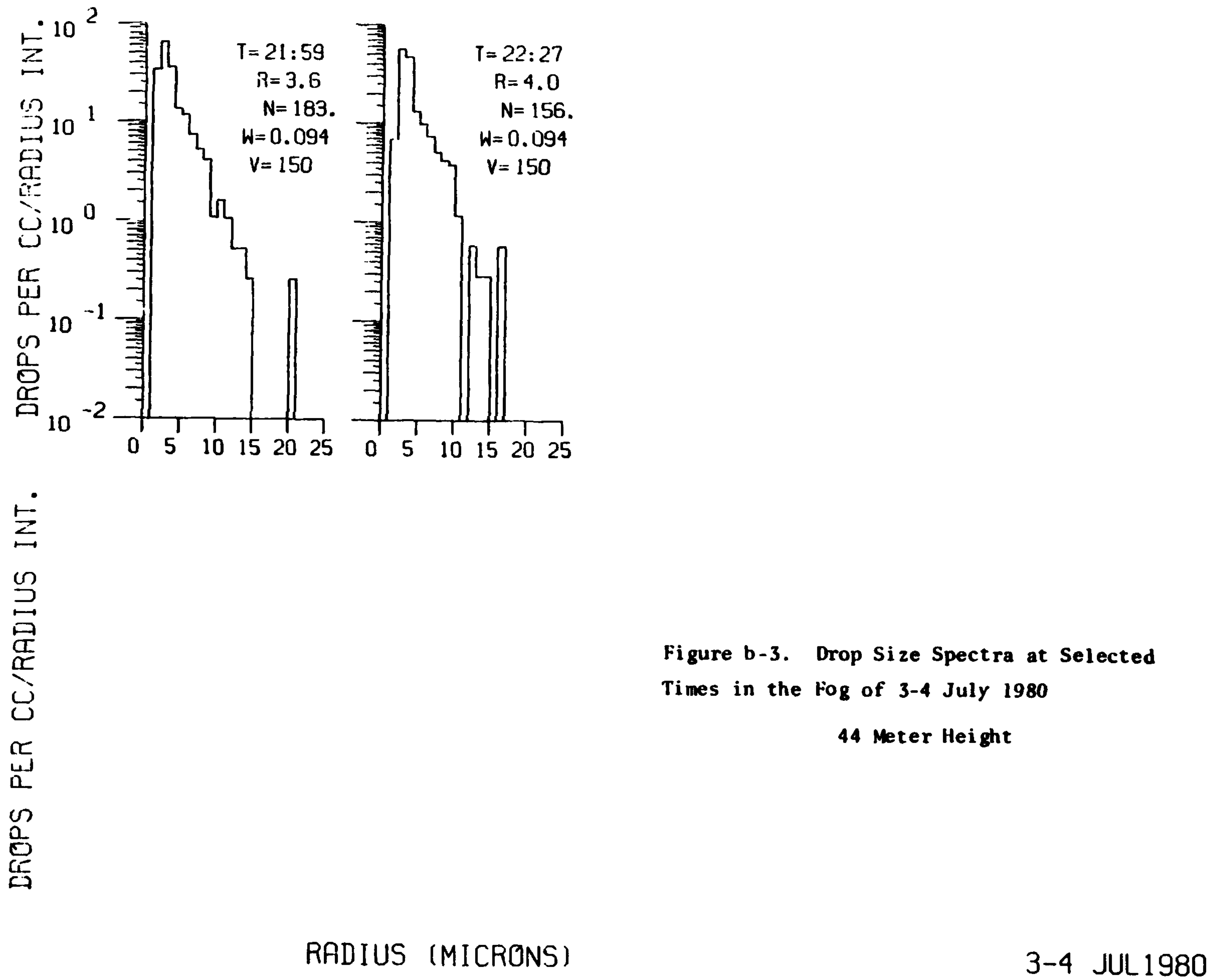

Figure b-3. Drop Size Spectra at Selected Times in the Fog of 3-4 July 1980

44 Meter Height

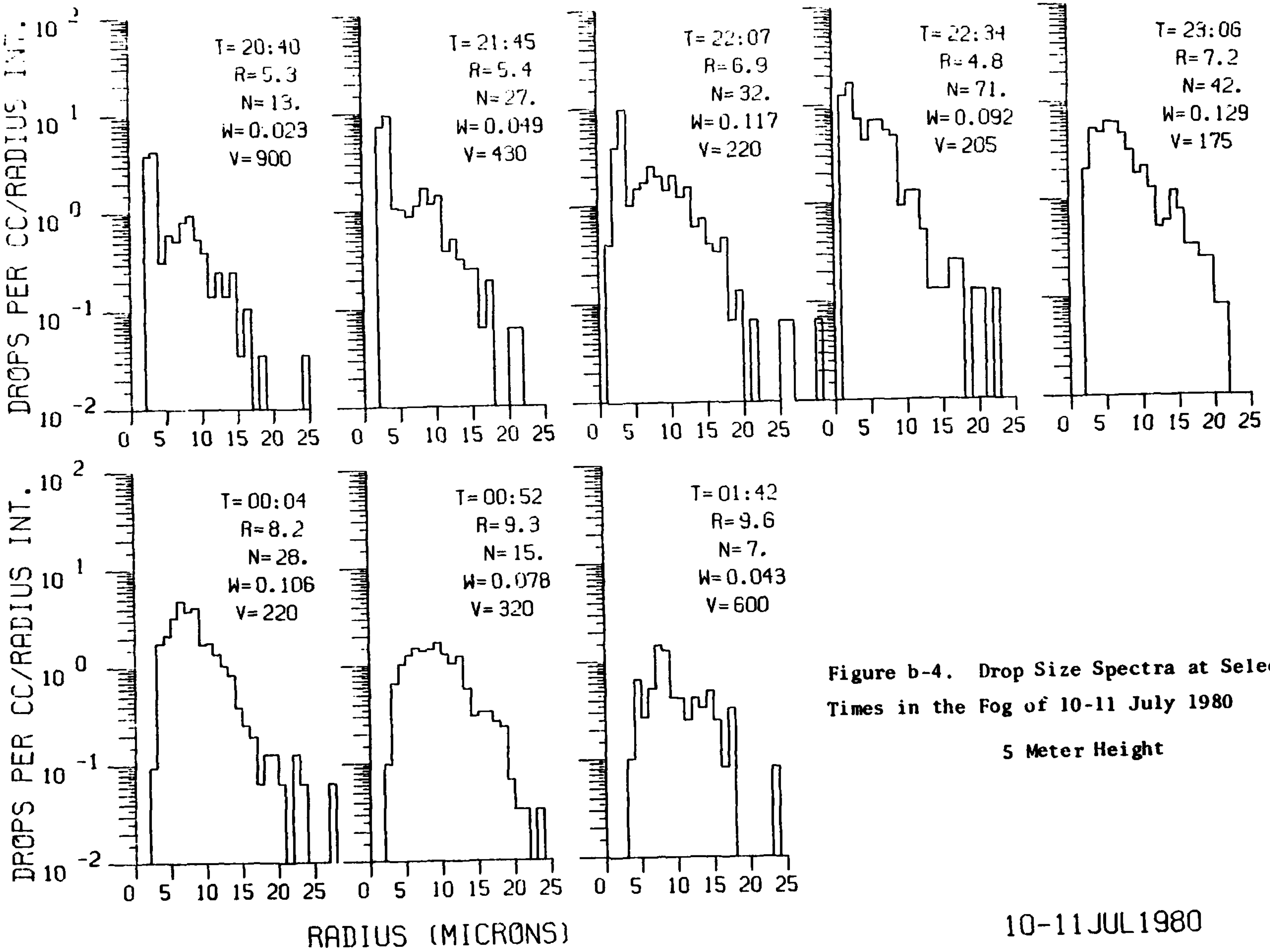

Figure b-4. Drop Size Spectra at Selected Times in the Fog of 10-11 July 1980

5 Meter Height

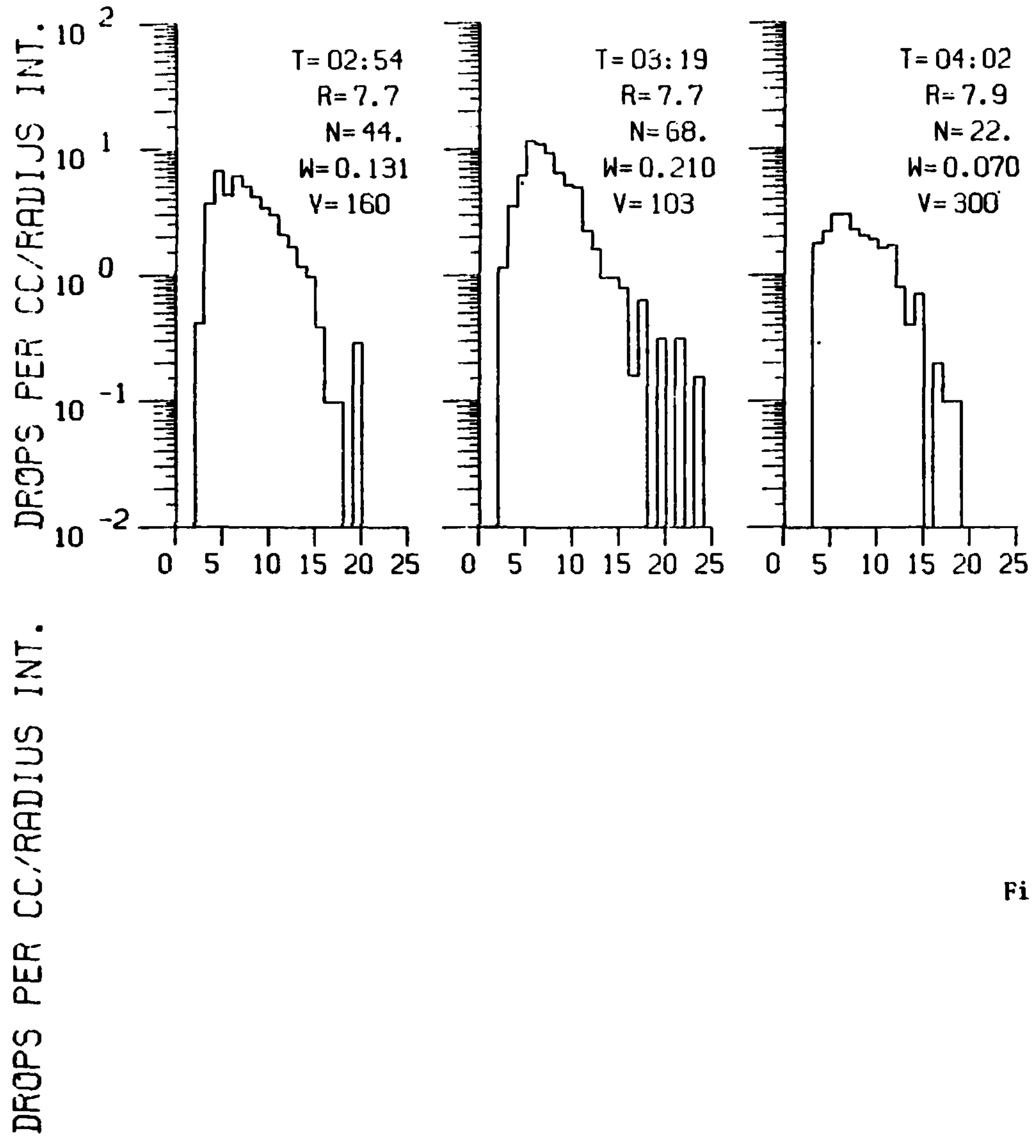

Figure b-4. (Cont.)

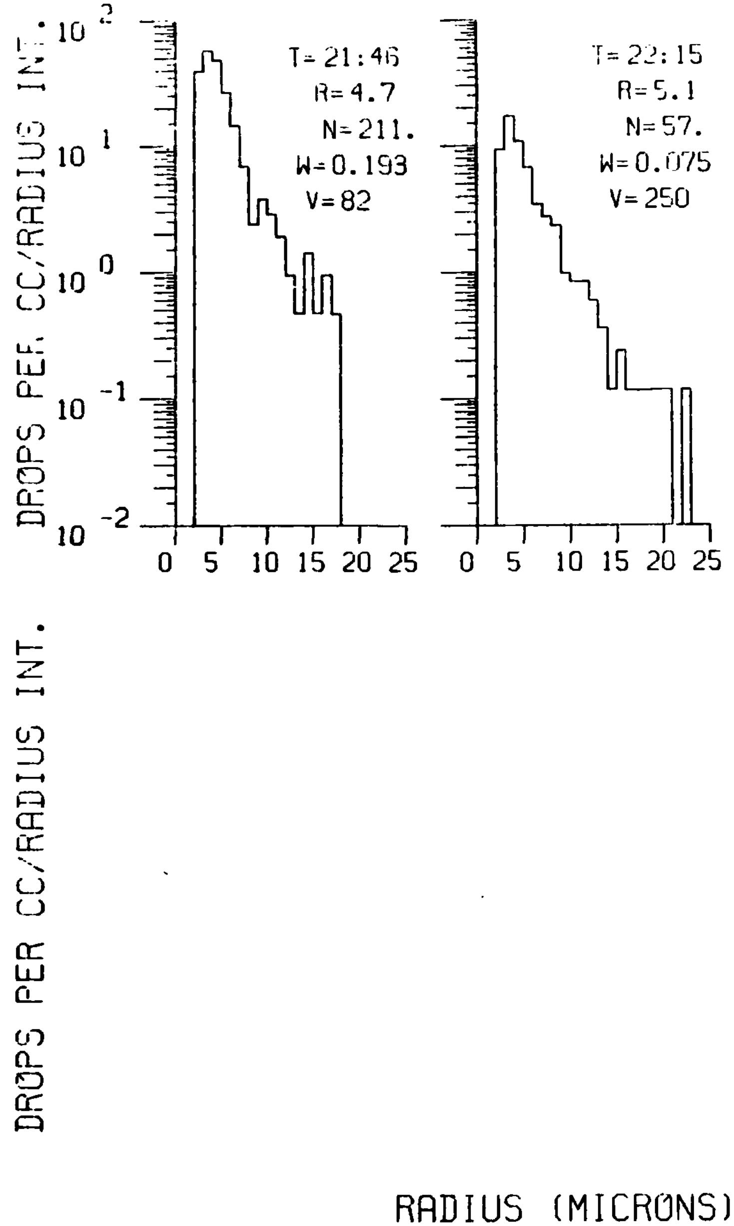

Figure b-5. Drop Size Spectra at Selected Times in the Fog of 10-11 July 1980

44 Meter Height

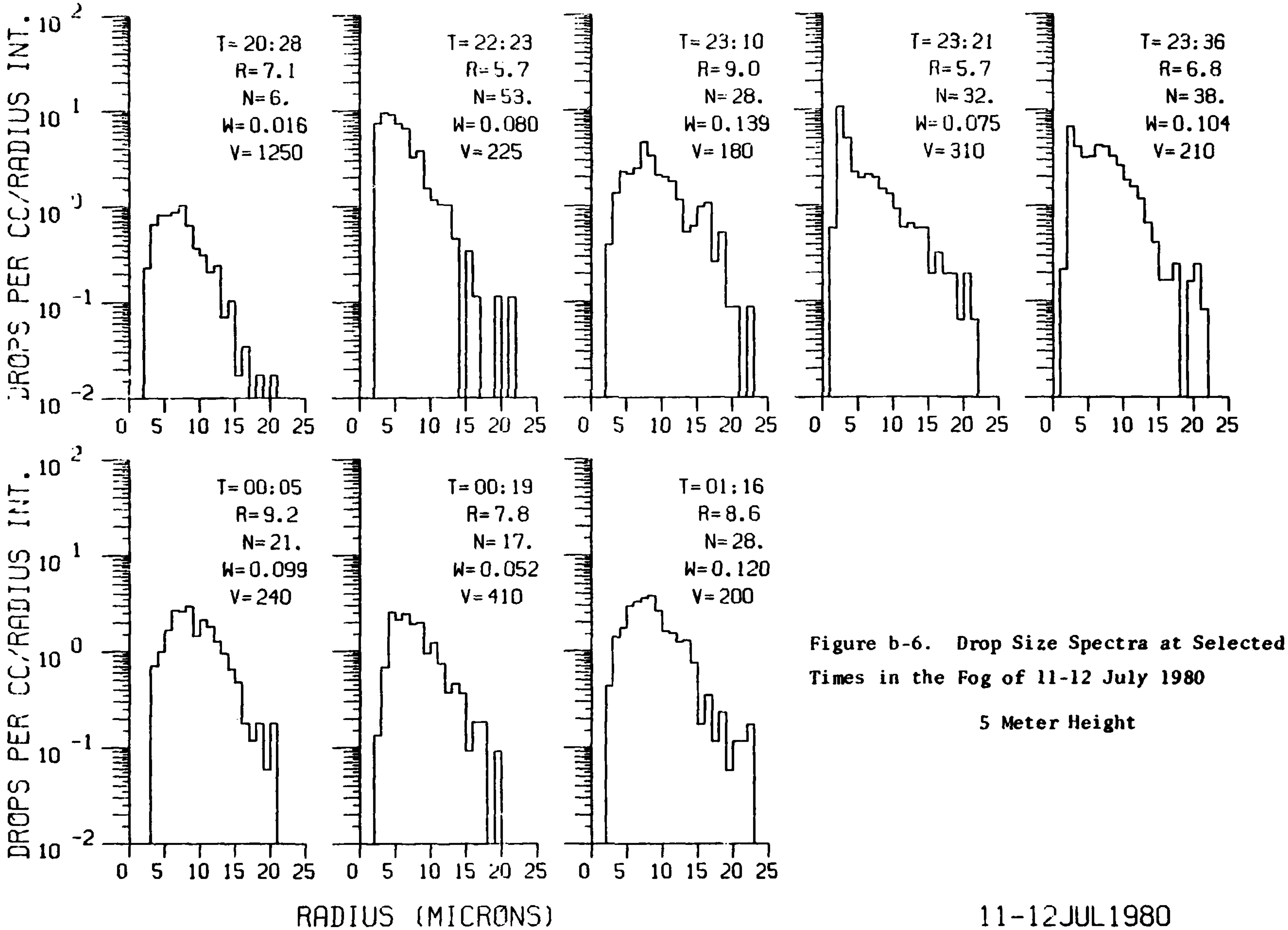

Figure b-6. Drop Size Spectra at Selected Times in the Fog of 11-12 July 1980

5 Meter Height

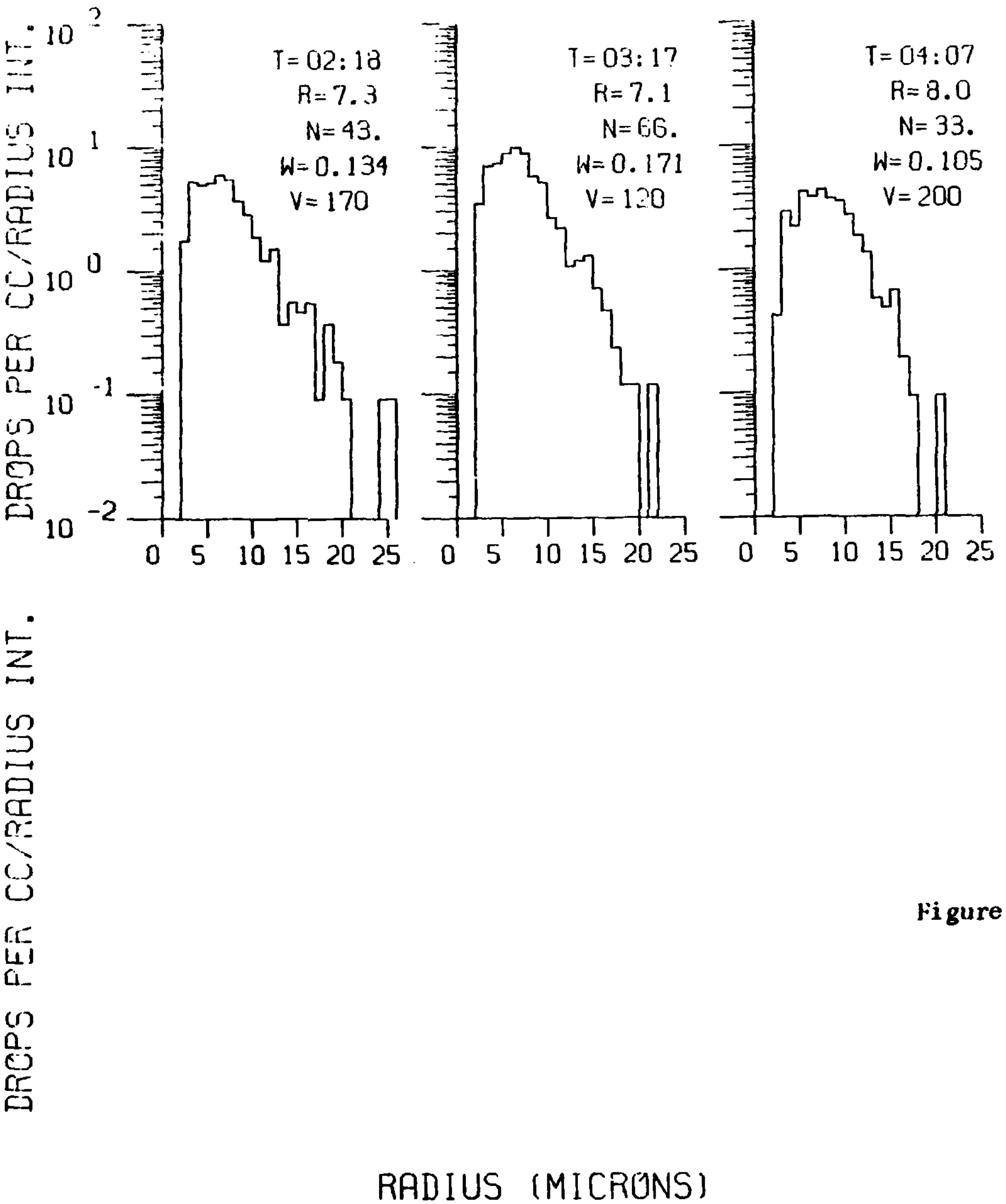

Figure b-6. (Cont.)

11-12JUL1980

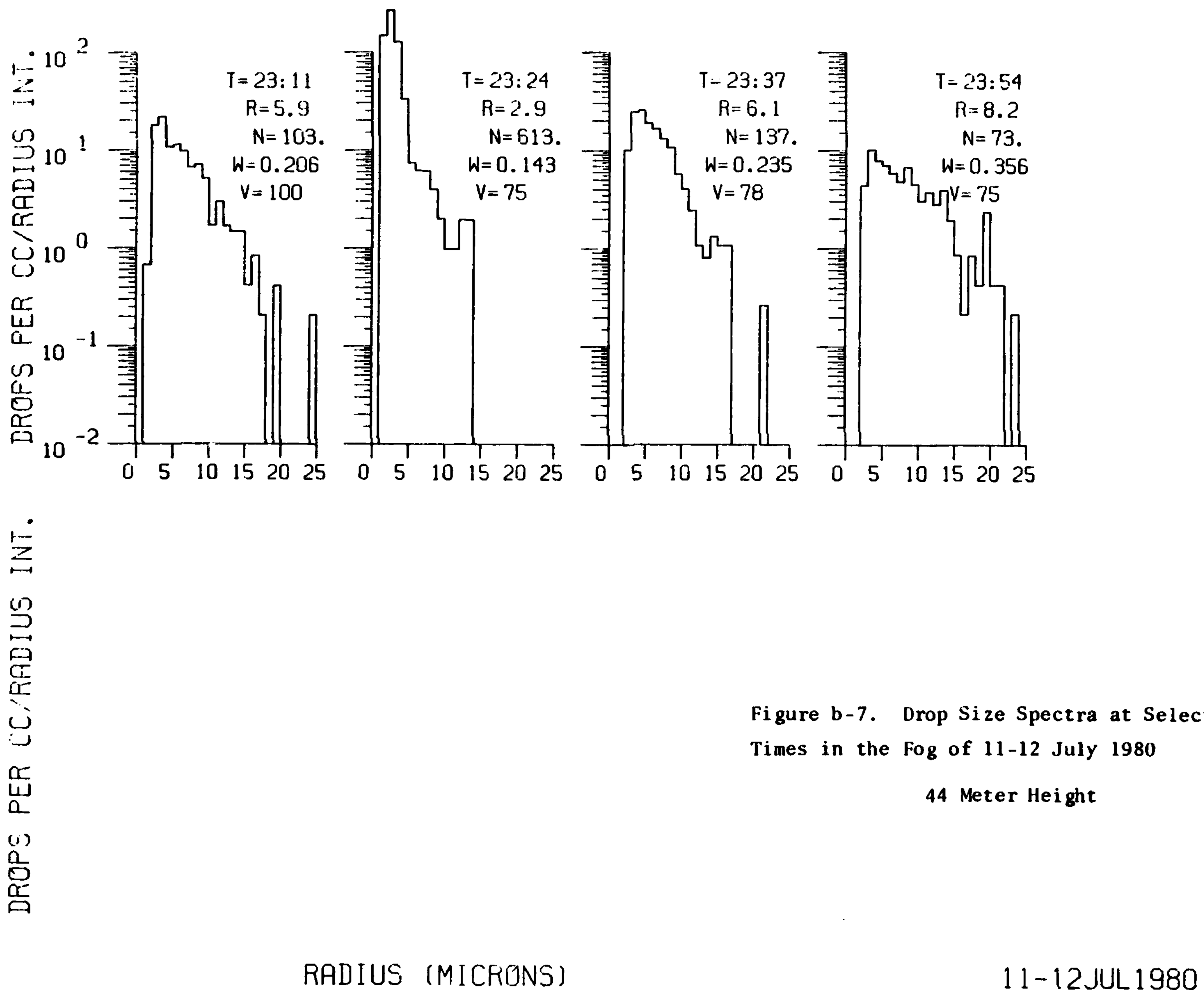

Figure b-7. Drop Size Spectra at Selected Times in the Fog of 11-12 July 1980

44 Meter Height

APPENDIX C

Low-level Air Temperature and Soil Temperature
Records for the Nights of 3-4, 4-5, 10-11 and 11-12 July 1980

Deep Advection Fog, 1900-0900 EDT

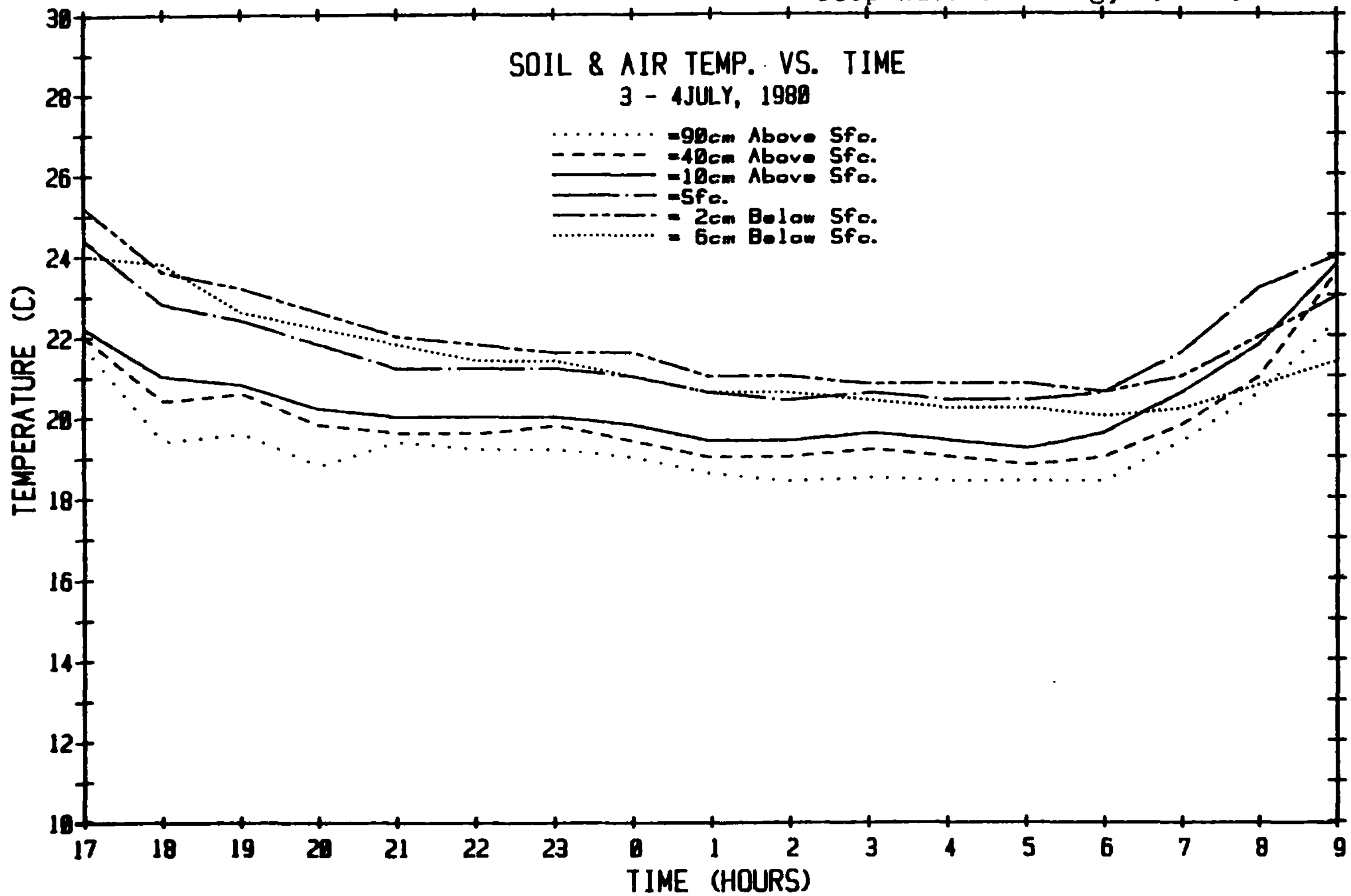

Figure C-1: Soil and Air Temperatures as Functions of Time at Otis AFB, 3-4 July 1980

Shallow Ground Fog, 0100-0630 EDT

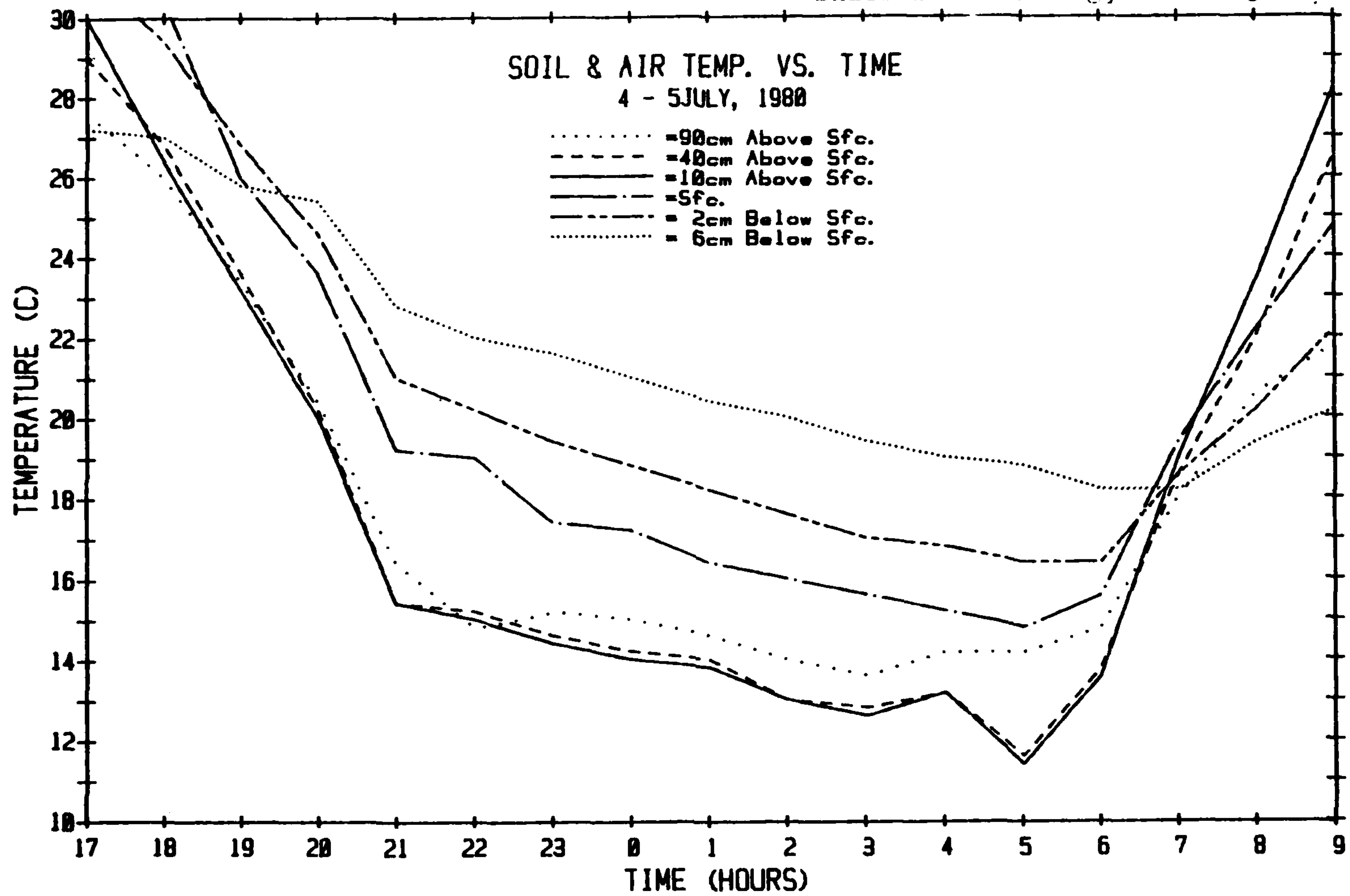

Figure C-2: Soil and Air Temperatures as Functions of Time at Otis AFB, 4-5 July 1980

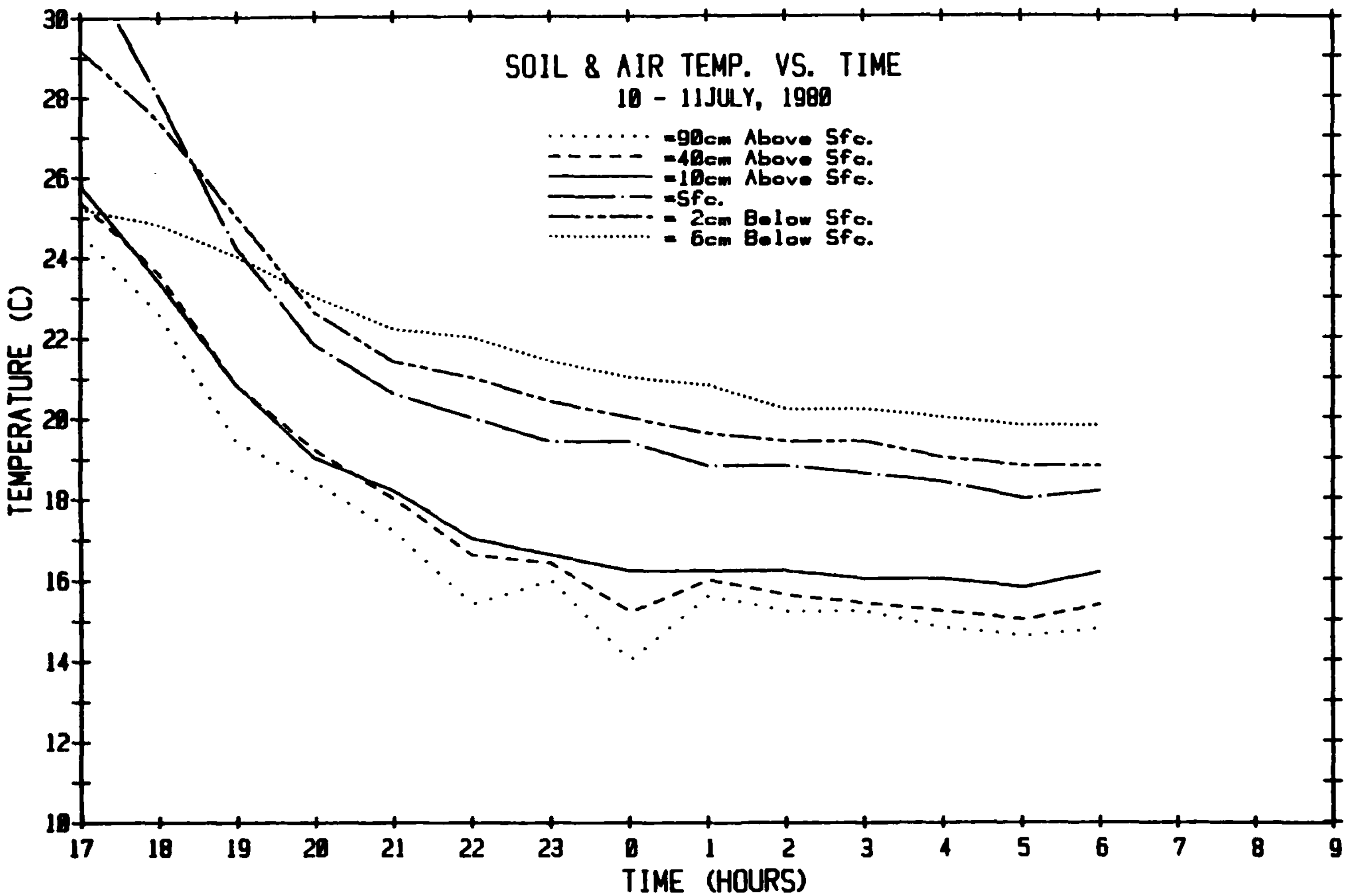

Figure C-3: Soil and Air Temperatures as Functions of Time at Otis AFB, 10-11 July 1980

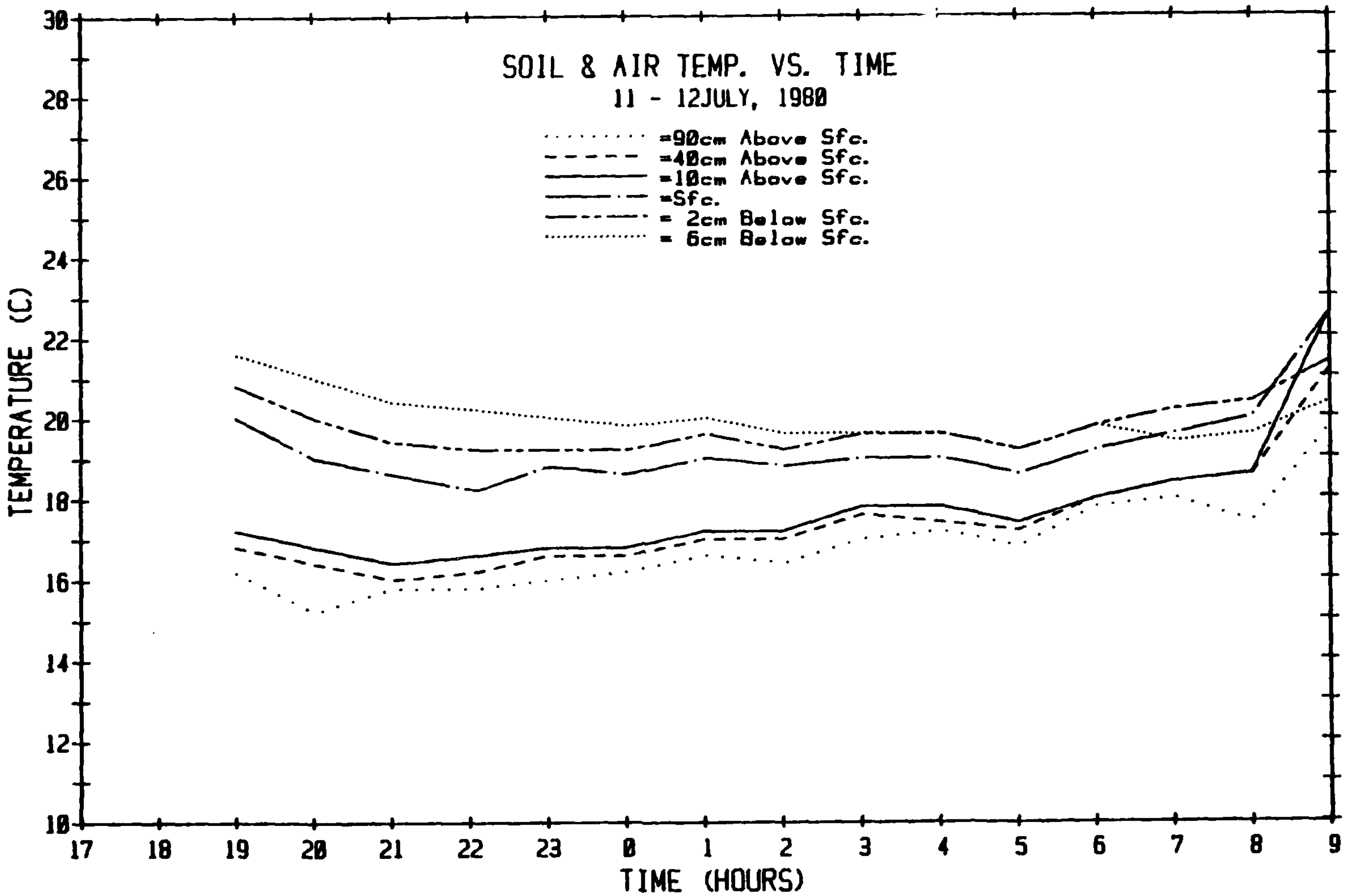

Figure C-4: Soil and Air Temperatures as Functions of Time at Otis AFB, 11-12 July 1980

APPENDIX D

Pre-Fog Aerosol Size Spectra Measured in the Early Evening Each Night During the Period 30 June to 17 July 1980 at Otis AFB

X TSI Electrical Aerosol Analyzer Data

O Royco OPC Data

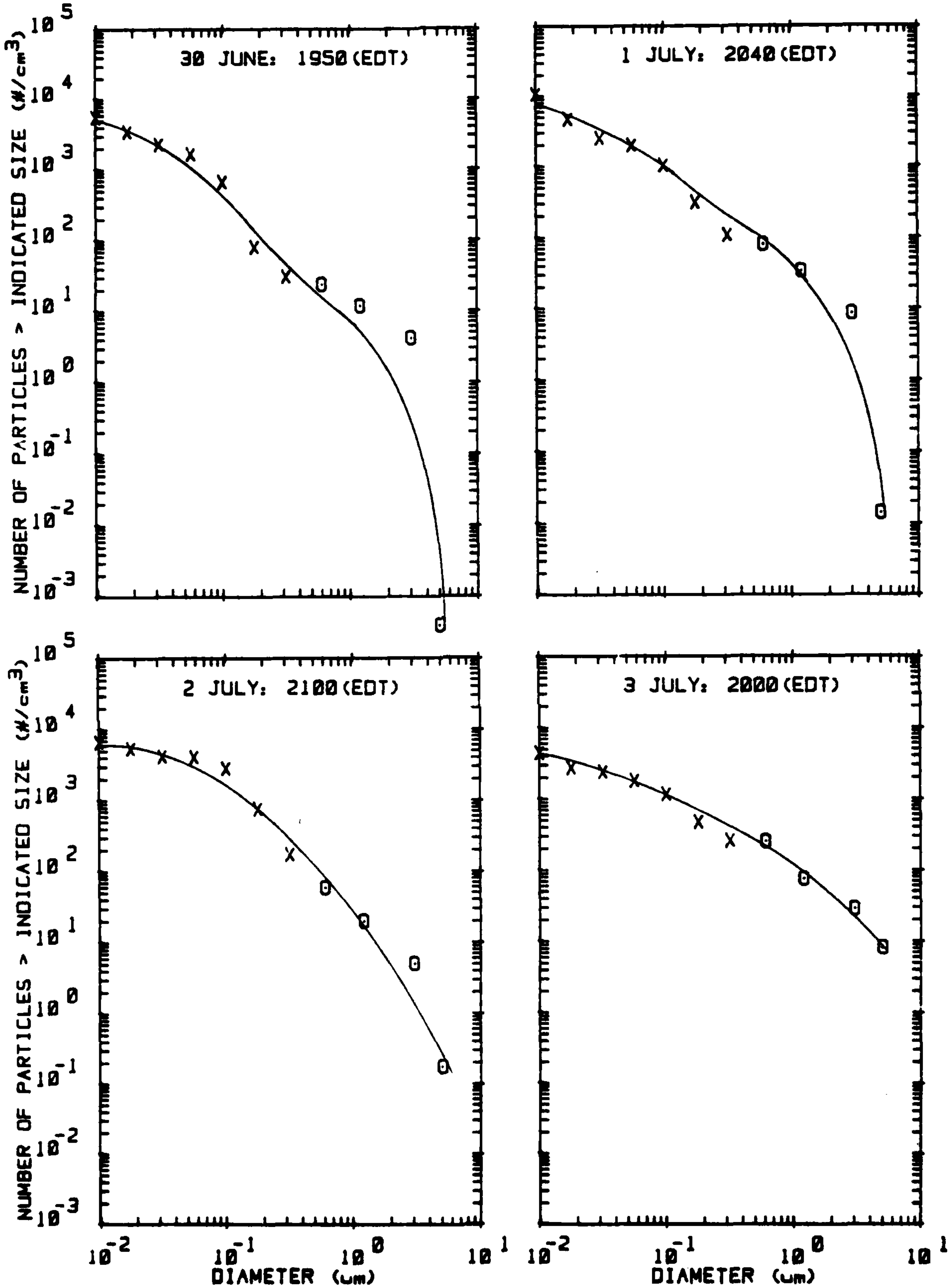

30 JUNE: 1950 (EDT)
1 JULY: 2040 (EDT)
2 JULY: 2100 (EDT)
3 JULY: 2000 (EDT)
NUMBER OF PARTICLES > INDICATED SIZE (#/cm³)
NUMBER OF PARTICLES > INDICATED SIZE (#/cm³)
10⁵
10⁴
10³
10²
10¹
10⁰
10⁻¹
10⁻²
10⁻³
10⁻²
10⁻¹
10⁰
10¹
DIAMETER (um)
DIAMETER (um)

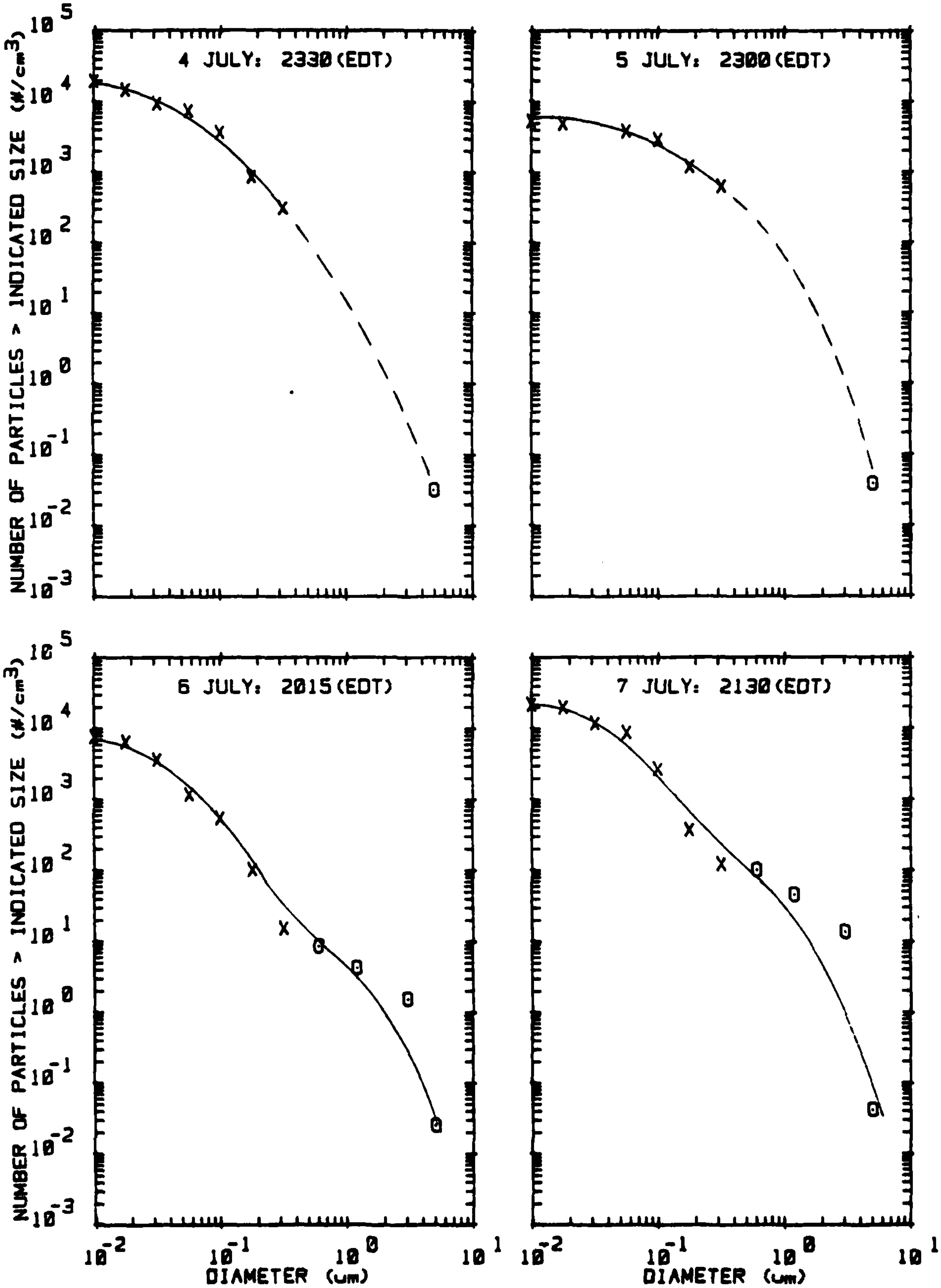
4 JULY: 2330 (EDT)
5 JULY: 2300 (EDT)
6 JULY: 2015 (EDT)
7 JULY: 2130 (EDT)
NUMBER OF PARTICLES > INDICATED SIZE (#/cm³)
DIAMETER (um)

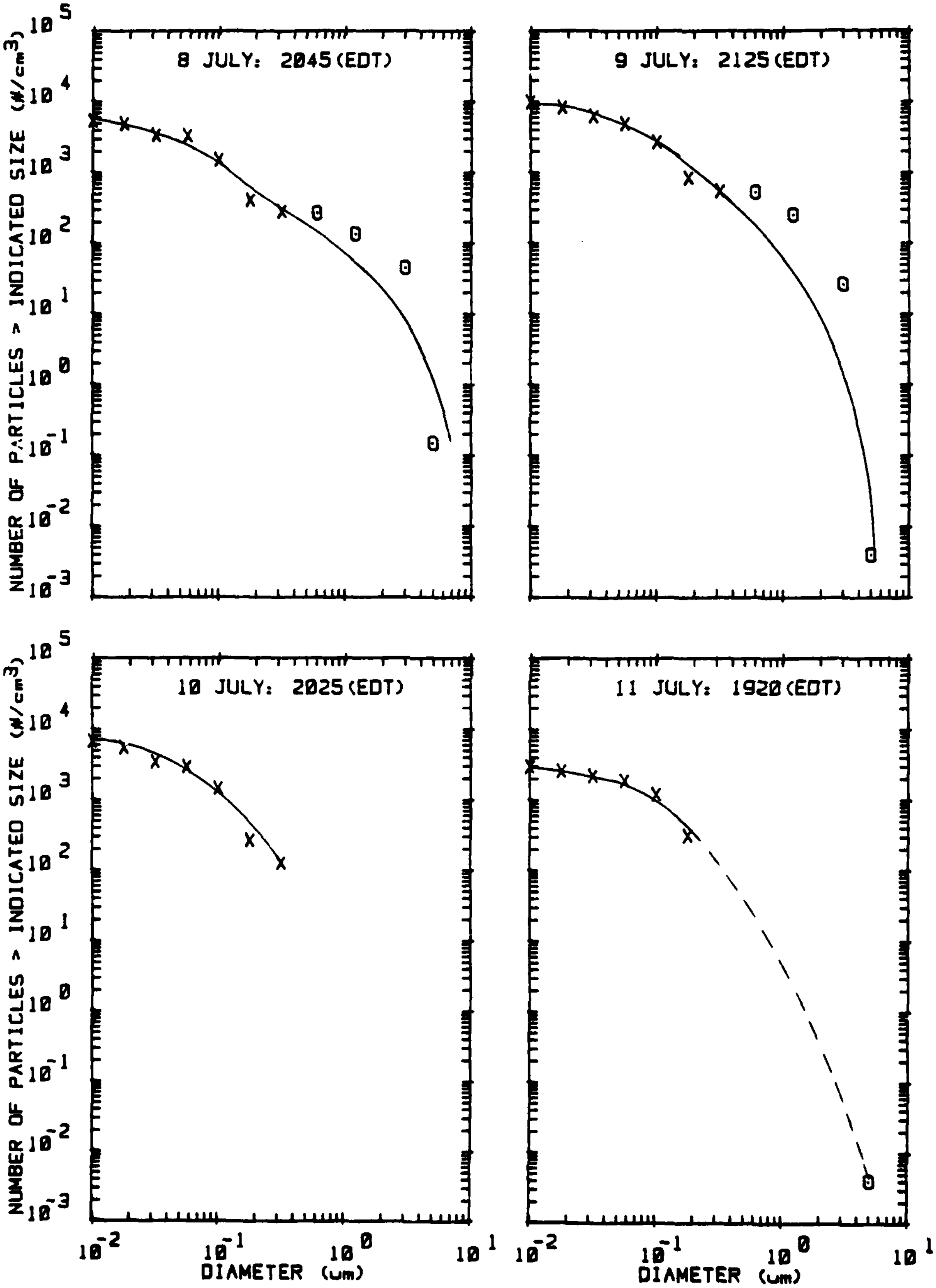
8 JULY: 2045 (EDT)
9 JULY: 2125 (EDT)
10 JULY: 2025 (EDT)
11 JULY: 1920 (EDT)
NUMBER OF PARTICLES > INDICATED SIZE (#/cm3)
DIAMETER (um)

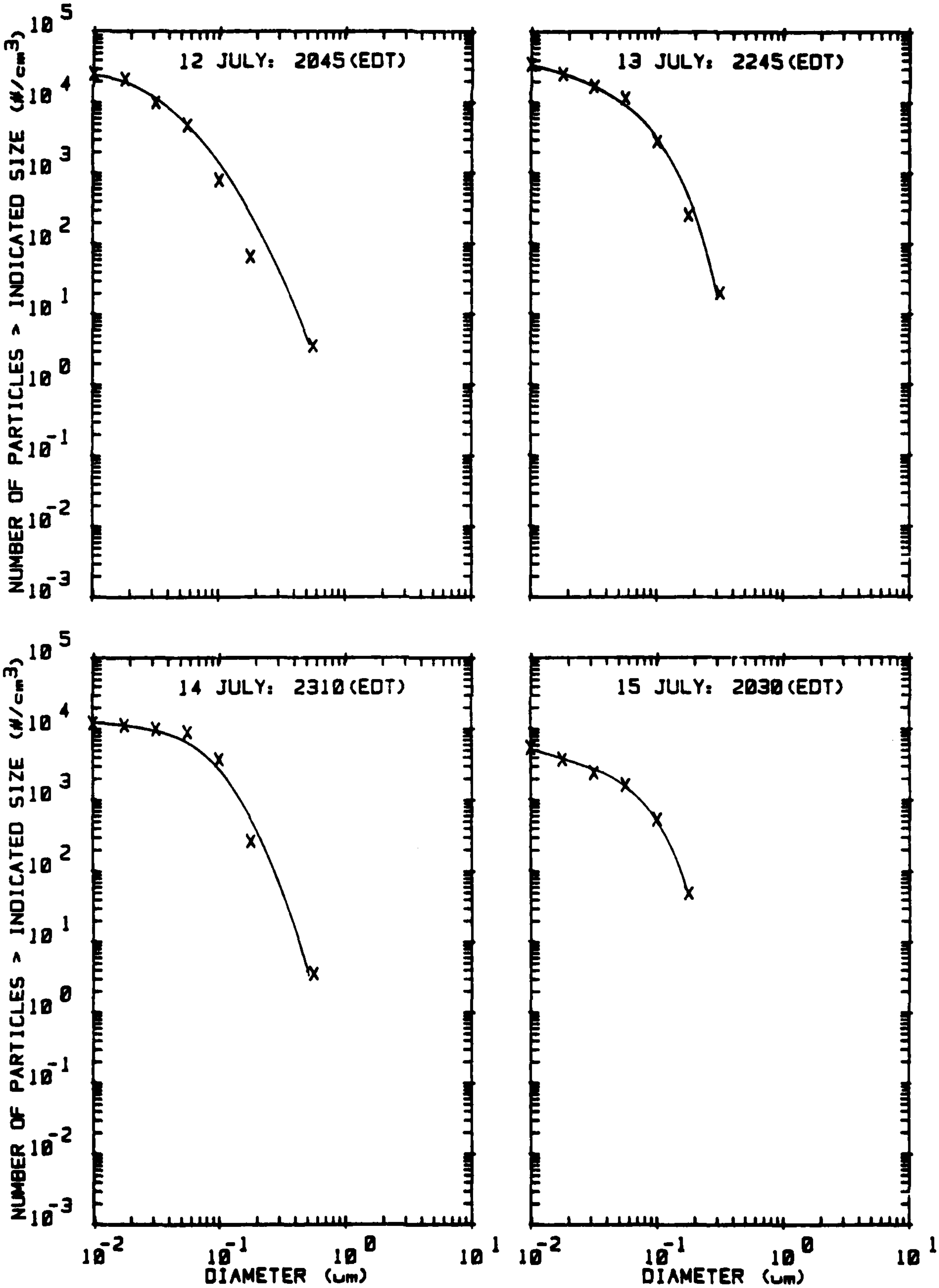
12 JULY: 2045(EDT)
13 JULY: 2245(EDT)
14 JULY: 2310(EDT)
15 JULY: 2030(EDT)
NUMBER OF PARTICLES > INDICATED SIZE (#/cm3)
DIAMETER (um)
10 5
10 4
10 3
10 2
10 1
10 0
10 -1
10 -2
10 -3

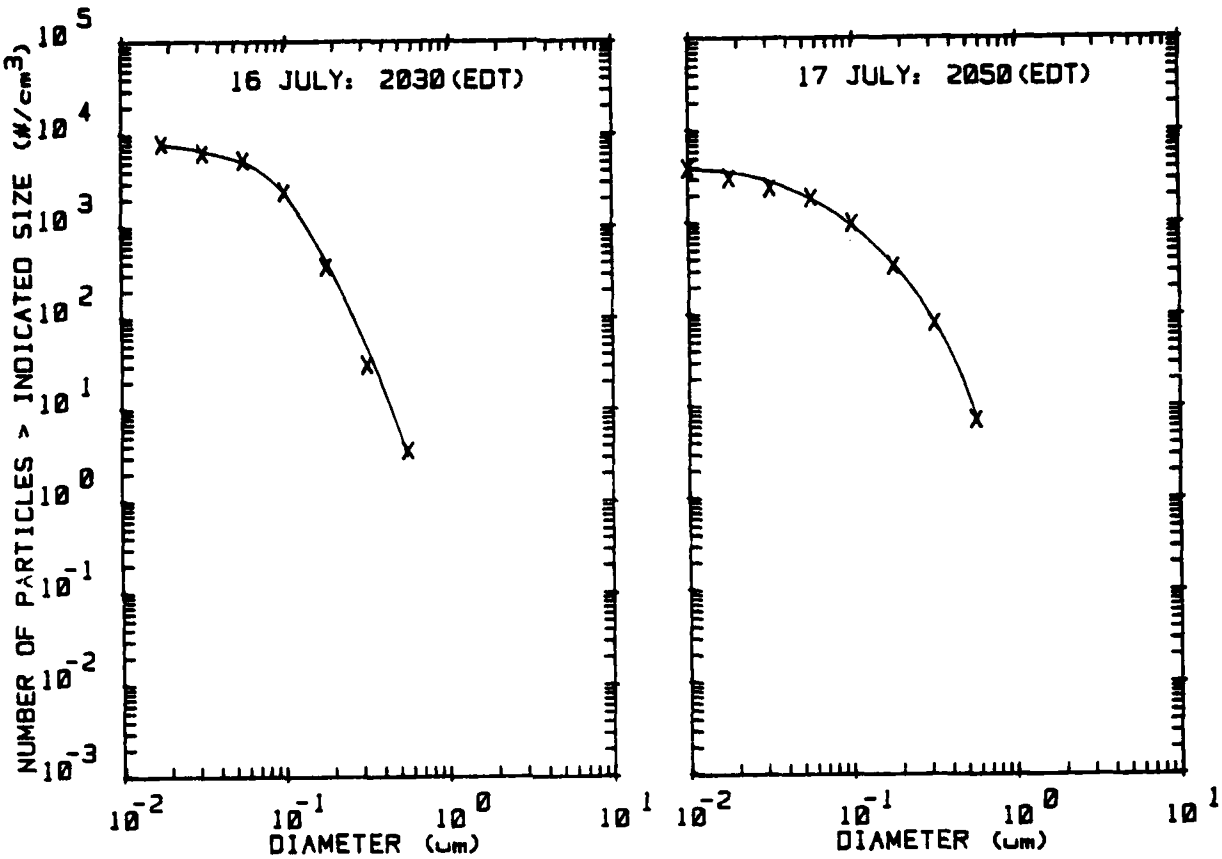

NUMBER OF PARTICLES > INDICATED SIZE (#/cm3)
16 JULY: 2030 (EDT)
17 JULY: 2050 (EDT)
DIAMETER (um)
DIAMETER (um)

APPENDIX E

Individual CCN Activity Spectra
Measured at Otis AFB, July 1980

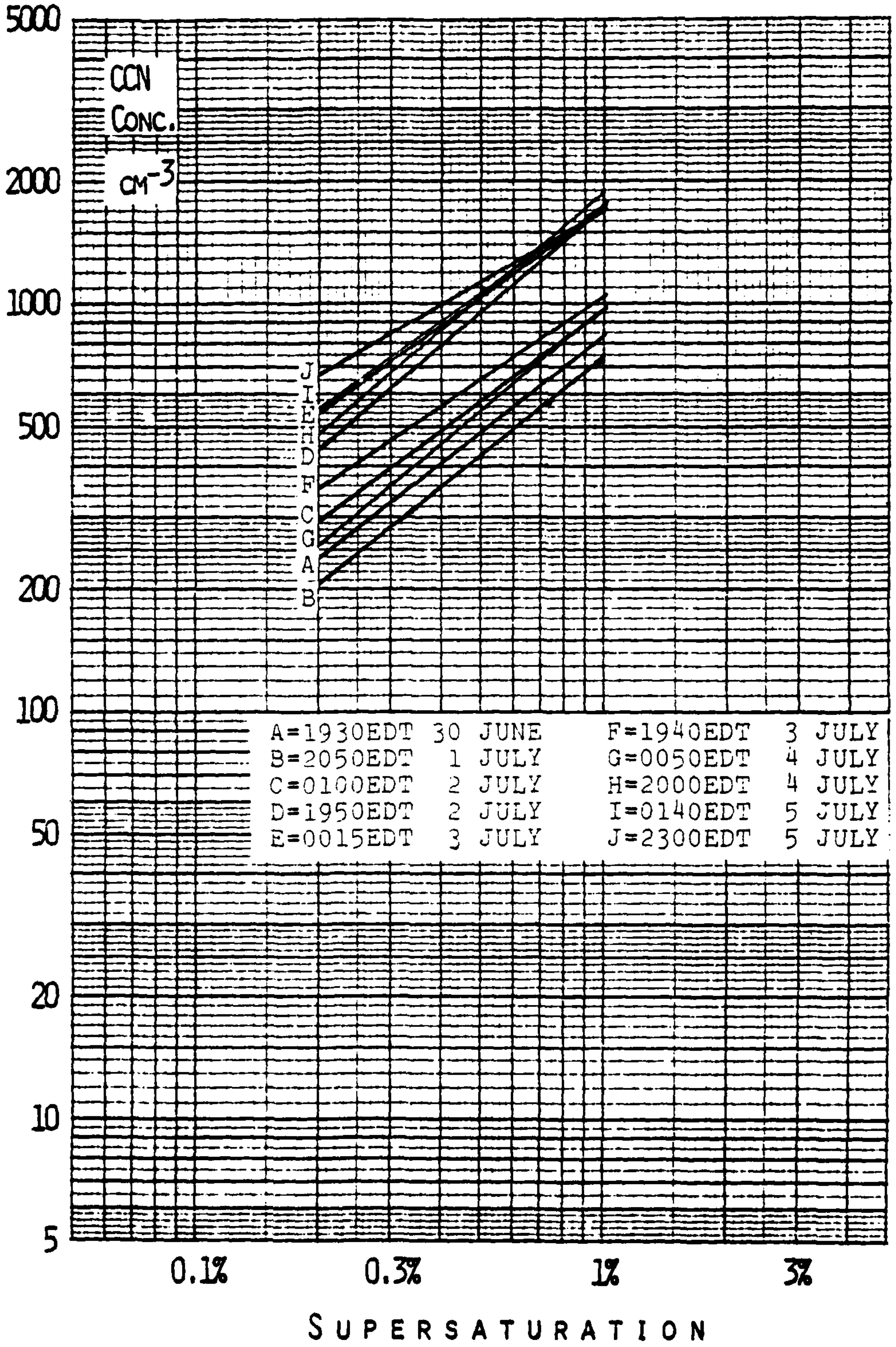

Figure E-1: CCN Activity Spectra at Otis AFB for the Period 1930EDT 30 June 1980 to 2300EDT 5 July 1980

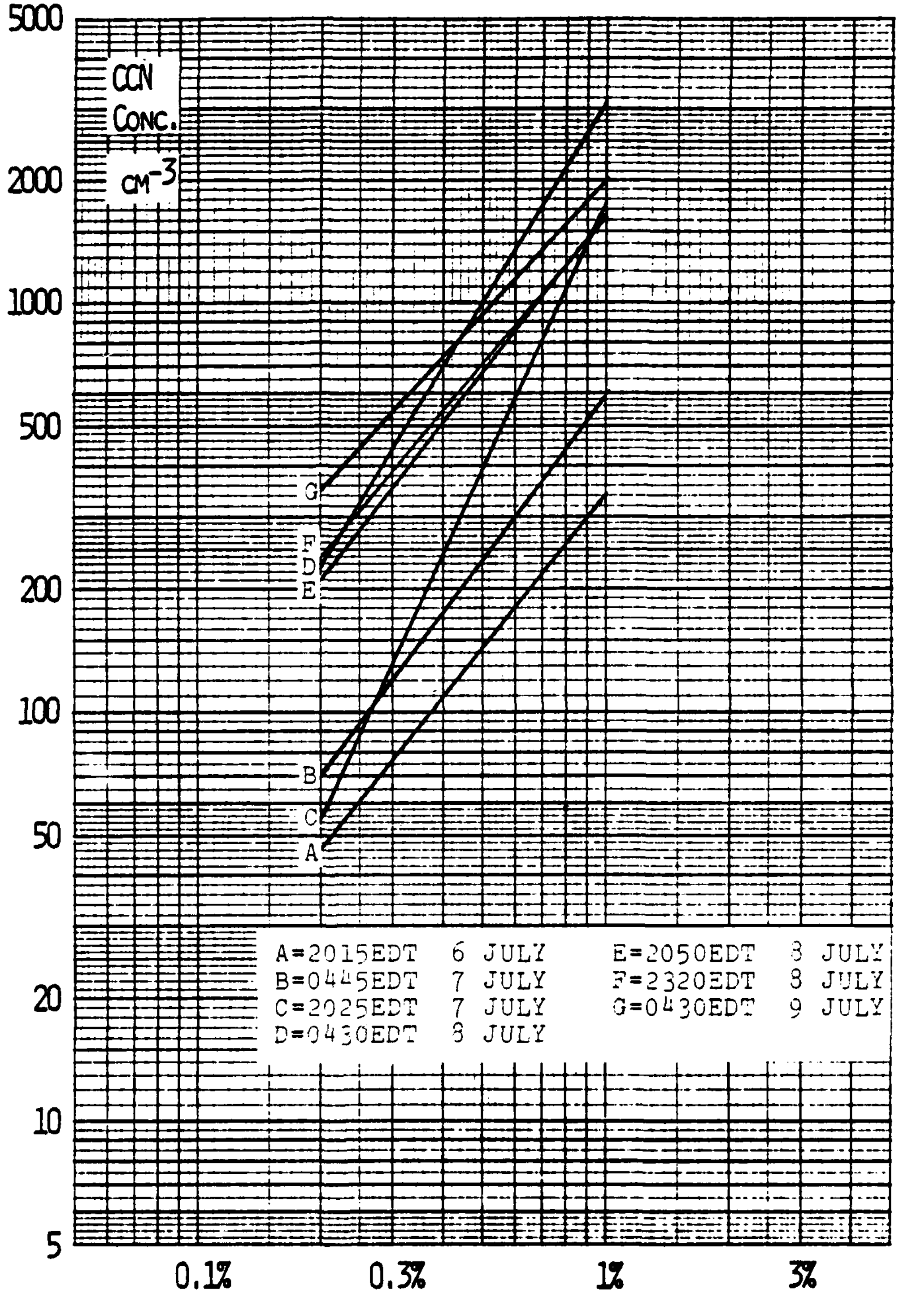

Figure E-2: CCN Activity Spectra at Otis AFB for the Period 2015EDT 6 July 1980 to 0430 9 July 1980

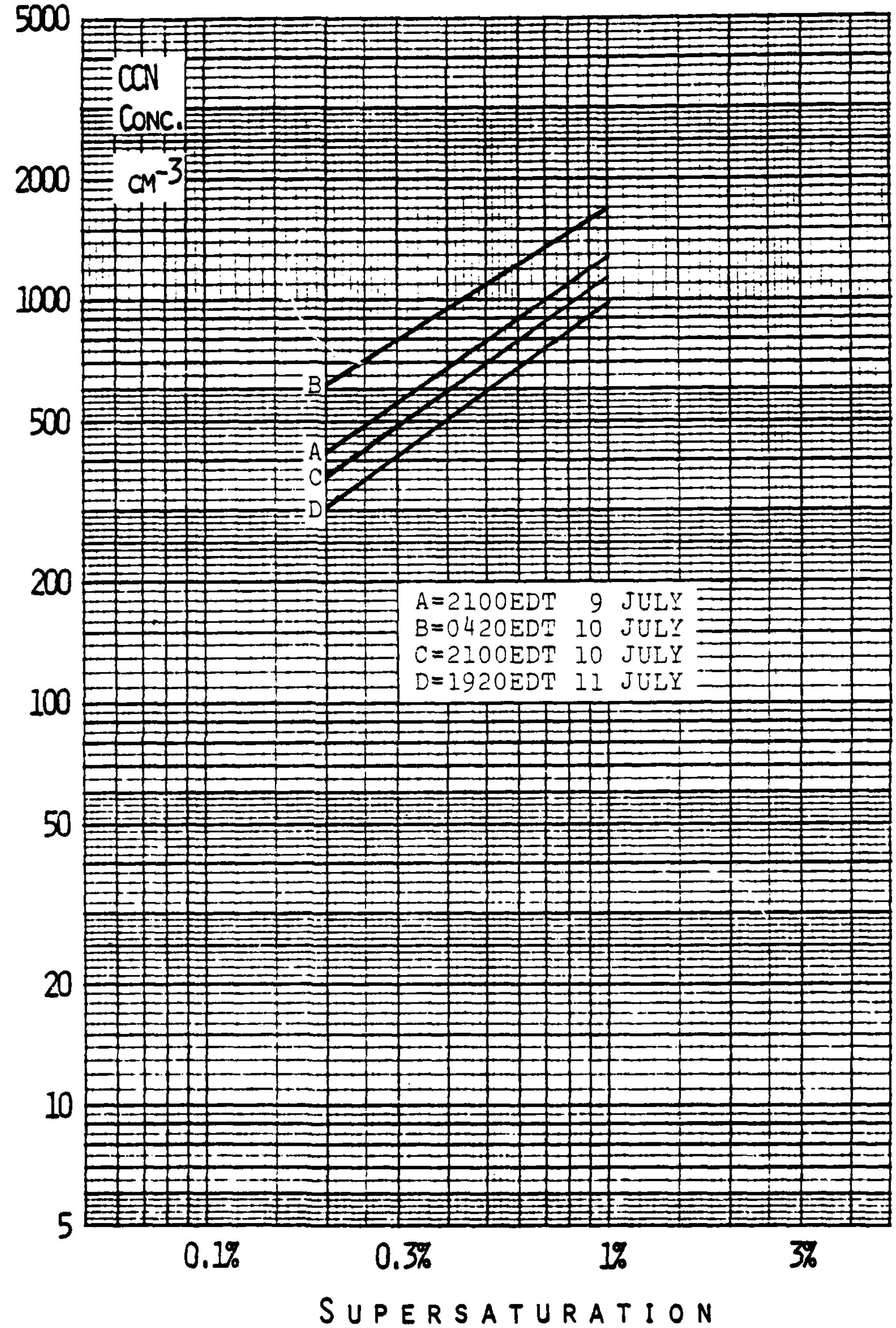

Figure E-3: CCN Activity Spectra at Otis AFB for the Period 2100EDT 9 July 1980 to 1920EDT 11 July 1980

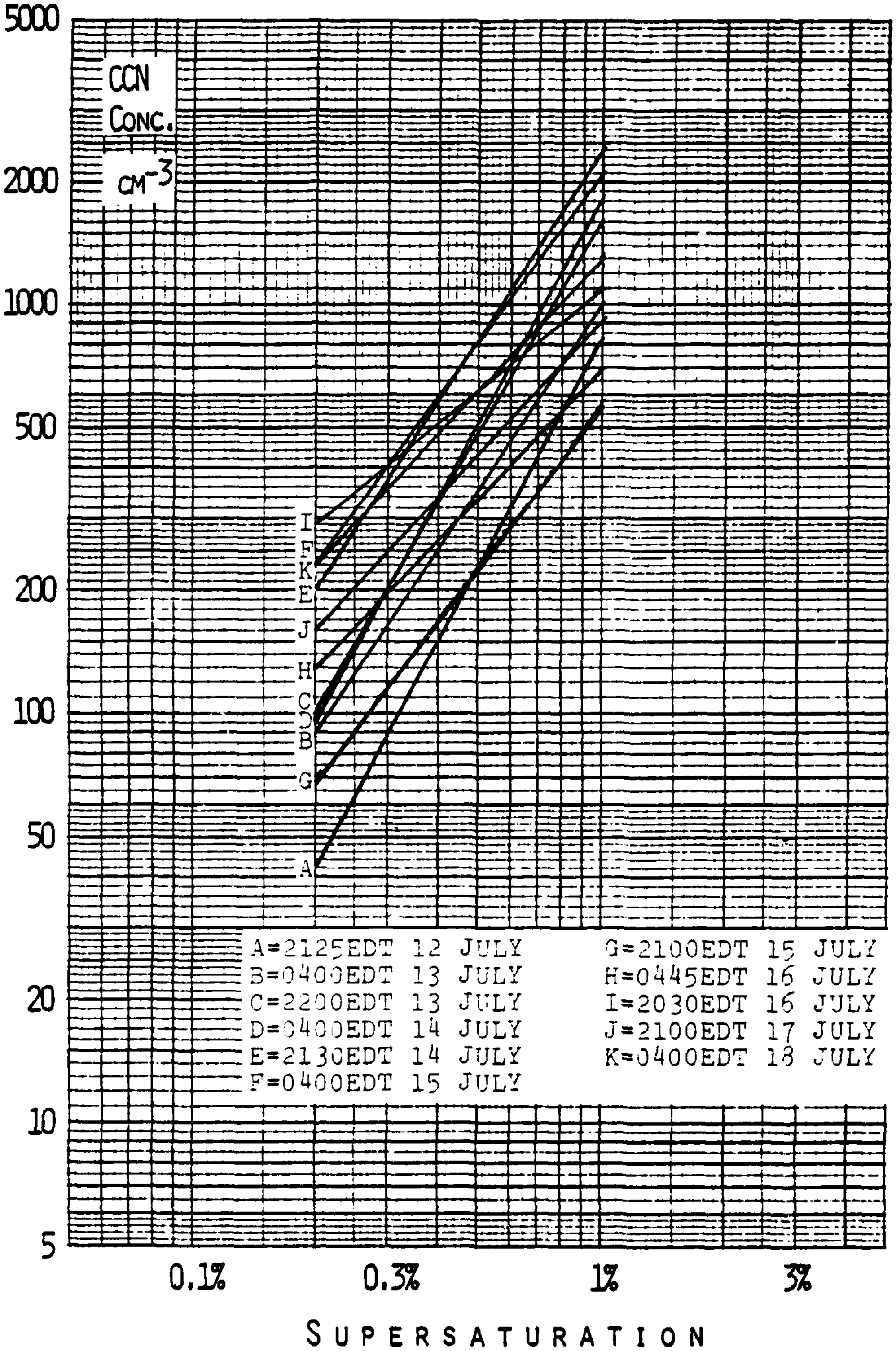

Figure E-4: CCN Activity Spectra at Otis AFB for the Period 2125EDT 12 July 1980 to 0400EDT 18 July 1980

DAT
FILM